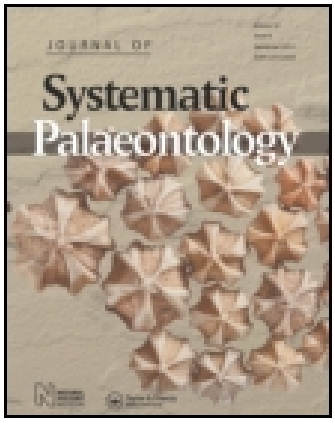

Journal of Systematic Palaeontology
Publication details, including instructions for authors and subscription information:
http://www.tandfonline.com/loi/tjsp20

Australohyaena antiqua (Mammalia, Metatheria, Sparassodonta), a large predator from the Late Oligocene of Patagonia

Analía M. Forasiepi[a], M. Judith Babot[b] & Natalia Zimicz[c]

[a] CONICET, IANIGLA, CCT-Mendoza, Av. Ruiz Leal s/n, 5500, Mendoza, Mendoza Province, Argentina

[b] Fundación Miguel Lillo, Miguel Lillo 251, 4000, San Miguel de Tucumán, Tucumán Province, Argentina

[c] CONICET, Cátedra de Geología Argentina y Sudamericana, Facultad de Ciencias Naturales, Universidad Nacional de Salta, Avenida Bolivia 5500, 4400, Salta Province, Argentina

Published online: 13 Jun 2014.

To cite this article: Analía M. Forasiepi, M. Judith Babot & Natalia Zimicz (2015) Australohyaena antiqua (Mammalia, Metatheria, Sparassodonta), a large predator from the Late Oligocene of Patagonia, Journal of Systematic Palaeontology, 13:6, 503-525, DOI: 10.1080/14772019.2014.926403

To link to this article: http://dx.doi.org/10.1080/14772019.2014.926403

Journal of Systematic Palaeontology, 2015
Vol. 13, No. 6, 503–525, http://dx.doi.org/10.1080/14772019.2014.926403

Australohyaena antiqua (Mammalia, Metatheria, Sparassodonta), a large predator from the Late Oligocene of Patagonia

Analía M. Forasiepi[a]*, M. Judith Babot[b] and Natalia Zimicz[c]

[a]*CONICET, IANIGLA, CCT-Mendoza, Av. Ruiz Leal s /n, 5500, Mendoza, Mendoza Province, Argentina;* [b]*Fundación Miguel Lillo, Miguel Lillo 251, 4000, San Miguel de Tucumán, Tucumán Province, Argentina;* [c]*CONICET, Cátedra de Geología Argentina y Sudamericana, Facultad de Ciencias Naturales, Universidad Nacional de Salta, Avenida Bolivia 5500, 4400, Salta Province, Argentina*

(Received 14 November 2013; accepted 24 March 2014; first published online 13 June 2014)

An almost complete skull of *Australohyaena antiqua* (Ameghino), from the Late Oligocene (Deseadan SALMA) of Cabeza Blanca, Chubut Province, Argentina is described and analysed. For more than a century, this species was represented by isolated teeth. The genus *Australohyaena* gen. nov. is proposed based on a phylogenetic reconstruction that demonstrates that *A. antiqua* is a Borhyaenidae (Mammalia, Sparassodonta), grouped with *Arctodictis* and *Borhyaena*, but not with *Pharsophorus lacerans*, the genus to which *antiqua* was formerly assigned. *A. antiqua* is recognized by several features on the skull, dentary and dentition. In addition, a short snout, large canines, deep jaw, reduced protocone and talonid determine *A. antiqua* as hypercarnivorous. A vaulted skull, well-developed temporal fossa and little difference on the jaw depth at p3 and m4, are suggestive of bone-cracker specializations. *A. antiqua* is within the largest Deseadan sparassodonts with a body mass of about 70 kg. Homoplasies are detected within borhyaenoids on lower molar cusps. The metaconid is lost within Sparassodonta, although *Pharsophorus* and borhyaenids retained the metaconid on m2–m4 or m2–m3.

http://zoobank.org/urn:lsid:zoobank.org:pub:EDB0575A-C1D9-4C17-B6EB-3D761D1D7DB3

Keywords: anatomy; phylogeny; palaeoecology; stem Marsupialia; Cenozoic; South America

Introduction

The Sparassodonta, a group of carnivorous metatherians, was a component of the native South American fauna. The group is recorded from the Palaeocene to the Pliocene. The Oligocene witnessed the start of the radiation of the lineages that predominated during the Neogene (Goin *et al.* 2010) and marked the decline of the largest members of the group, the Proborhyaenidae, which became extinct by the Deseadan age (Bond & Pascual 1983; Babot 2005). The overall diversity of the Sparassodonta reached a peak of eight known species in the Oligocene, represented by hypercarnivores of all sizes (Zimicz 2012; Prevosti *et al.* 2013). Deseadan sparassodonts have been recovered from several localities spread over different latitudes of South America. The north of the continent produced sparassodonts from Tremembé, Brazil (Borhyaenidae indet.; Soria & Alvarenga 1989) and Salla, Bolivia (*Fredszalaya hunteri*, *Notogale mitis*, *Paraborhyaena boliviana*, *Pharsophorus lacerans* and *Sallacyon hoffstetteri*; Villarroel & Marshall 1982; Petter & Hoffstetter 1983; Shockey & Anaya 2008). Southern South America provided two non-Patagonian sites. From Paso del Cuello (Uruguay), Mones & Ubilla (1978) described *Proborhyaena* cf. *P. gigantea*; and from Quebrada Fiera (Mendoza, Argentina), Bond & Pascual (1983) described *Proborhyaena gigantea* and Cerdeño (2011) mentioned the occurrence of *Pharsophorus* sp. In Patagonia, Deseadan sparassodonts were mainly collected from Cabeza Blanca and Rinconada de los López (including Scarritt Pocket). The Cabeza Blanca locality provided *Pharsophorus lacerans*, *Pharsophorus tenax*, *Notogale mitis*, *Notogale*(?) *tenuis* and *Proborhyaena gigantea*. This locality was also the source of the specimen studied here. Rinconada de los López yielded cf. *Pharsophorus* sp. and *Proborhyaena gigantea* (Ameghino 1897; Loomis 1914; Chaffee 1952; Marshall 1978; Patterson & Marshall 1978). A few other Patagonian localities such as Laguna La Bombilla, Laguna Payahilé, La Flecha, and Pico Truncado (Santa Cruz Province) have provided fragmentary remains.

In this contribution we analyse an almost complete skull of a borhyaenid (UNPSJB PV 113) from the Cabeza Blanca locality (Sarmiento Formation; Deseadan Age, Late Oligocene). We provide a complete anatomical description of the specimen, review the taxonomy of *Pharsophorus*(?) *antiquus*, give an emended diagnosis of the species, propose a hypothesis of its phylogenetic relationships, and analyse some palaeobiological aspects (diet and body mass).

*Corresponding author. Email: borhyaena@hotmail.com

Geographical and stratigraphical location

The locality of Cabeza Blanca is one of the richest sites with a Deseadan fauna in Patagonia (Loomis 1914; Reguero & Escribano 1996). First explored by Carlos Ameghino between 1894 and 1896, Cabeza Blanca is located 5 km south-west of the Estancia Venter (45° 13′ 55″ S, 67° 28′ 07″ W), east of the Chico River, Escalante Department, Chubut Province, Argentina (Fig. 1A). The stratigraphical sequence exposed at Cabeza Blanca is composed of marine and continental sediments. The fossiliferous levels where the mammals come from have been referred to the Sarmiento Formation. At Cabeza Blanca, the Sarmiento Formation has been subdivided into two. The basal levels are composed of white to grey claystones and have Casamayoran mammals (Fig. 1B). The overlying levels are variable in grain size and include green, grey and white sandstones and claystones, with tuff content. Fossil vertebrates have been discovered throughout this sequence and are assigned to the Deseadan Age (Reguero & Escribano 1996). Specimen UNPSJB PV 113 comes from the fossiliferous middle levels of the Deseadan Sarmiento Formation (Abril Monica, pers. comm.; Fig. 1B). The absolute date of the Deseadan SALMA was estimated to be between 30−23 Ma (Dunn *et al.* 2012).

Material and methods

The nomenclature for the descriptions follows veterinary text books (e.g. Schaller 1992) and publications on metatherians (de Muizon 1998; Wible 2003). The hypotympanic sinus is "the part of the tympanic cavity that contains none of its principal elements, including the auditory ossicles and the fenestrae in the periotic" (Van der Klaauw 1931, p. 19). Following de Muizon (1998), the hypotympanic sinus in the Sparassodonta can be formed by: (a) the expansion of the alisphenoid, squamosal and petrosal, or some of these bones, assuming that the spaces are homologous even when different bones surround it; or (b) the anteroventral expansion of the alisphenoid tympanic process (de Muizon 1998). The nomenclature for the dentition follows Hershkovitz (1982), Marshall (1978) and de Muizon (1998). The orientation of the teeth follows the terminology of Smith & Dodson (2003).

The general anatomy of UNPSJB PV 113 is similar to other sparassodonts (e.g. *Borhyaena*, *Arctodictis*, *Callistoe*; Sinclair 1906; Babot 2005; Forasiepi 2009). Bone contacts and sutures are mentioned in the description only if differences exist with the compared taxa, listed in the Supplemental Material.

The phylogenetic relationships between sparassodont species has been tested through a parsimony analysis conducted with the program TNT 1.1 (Goloboff *et al.* 2008a, b), under equal and implied weighted characters. Because uncertainties exist in the homologies of the talonid cusps in Borhyaenidae, the primary homologies (the conjectural homologies based on similarity) were tested following de Pinna (1991) and recent examples with this methodological approach (O'Meara & Thompson 2014). The secondary homologies (primary homologies that have been evaluated against the framework of a general pattern; de Pinna 1991) have been tested by congruence, coding as uncertainties (?) conflicting characters and constructing new phylogenetic trees.

Linear measurements, morphometric indexes and body mass were calculated with the aim of characterizing the ecomorph space (Werdelin 1989; Van Valkenburgh 2007) of *Australohyaena antiqua*. Measurements are in millimetres and are provided in the Supplemental Material.

Institutional abbreviations

FMNH: Field Museum of Natural History, Chicago, USA; **MACN A**: Museo Argentino de Ciencias Naturales 'Bernardino Rivadavia', Ameghino Collection, Buenos Aires, Argentina; **PVL**: Paleontología de Vertebrados Lillo, Instituto Miguel Lillo, Tucumán, Argentina; **UNPSJB PV**: Universidad Nacional de La Patagonia 'San Juan Bosco', Paleontología de Vertebrados, Comodoro Rivadavia, Argentina; **UF**: University of Florida, Vertebrate Paleontology Division, Florida Museum of Natural History, Gainesville, FL, USA; **YPM PU**: Yale Peabody Museum, collection of Princeton University, New Haven, CT, USA.

Anatomical abbreviations

Capital and lower case letters refer to upper and lower teeth, respectively: C/c, canine; I/i, incisor; M/m, molar; P/p, premolar.

Systematic palaeontology

Subclass **Metatheria** Huxley 1880
Order **Sparassodonta** Ameghino 1894
Family **Borhyaenidae** Ameghino 1894
Genus ***Australohyaena*** gen. nov.

1894 ?*Borhyaena antiqua* Ameghino: 655.
1897 *Proborhyaena antiqua* Ameghino: 502.
1914 *Proborhyaena antiqua* Ameghino; Loomis: 219.
1978 *Pharsophorus*(?) *antiquus* (Ameghino); Marshall: 36, fig. 7, table 3.

Type species. *Australohyaena antiqua* (Ameghino 1894), MACN A 52-532, a nearly complete isolated right upper canine.

Diagnosis. As for the type and only known species.

Derivation of name. *Australo-* refers to south, given the endemic South American distribution of sparassodonts;

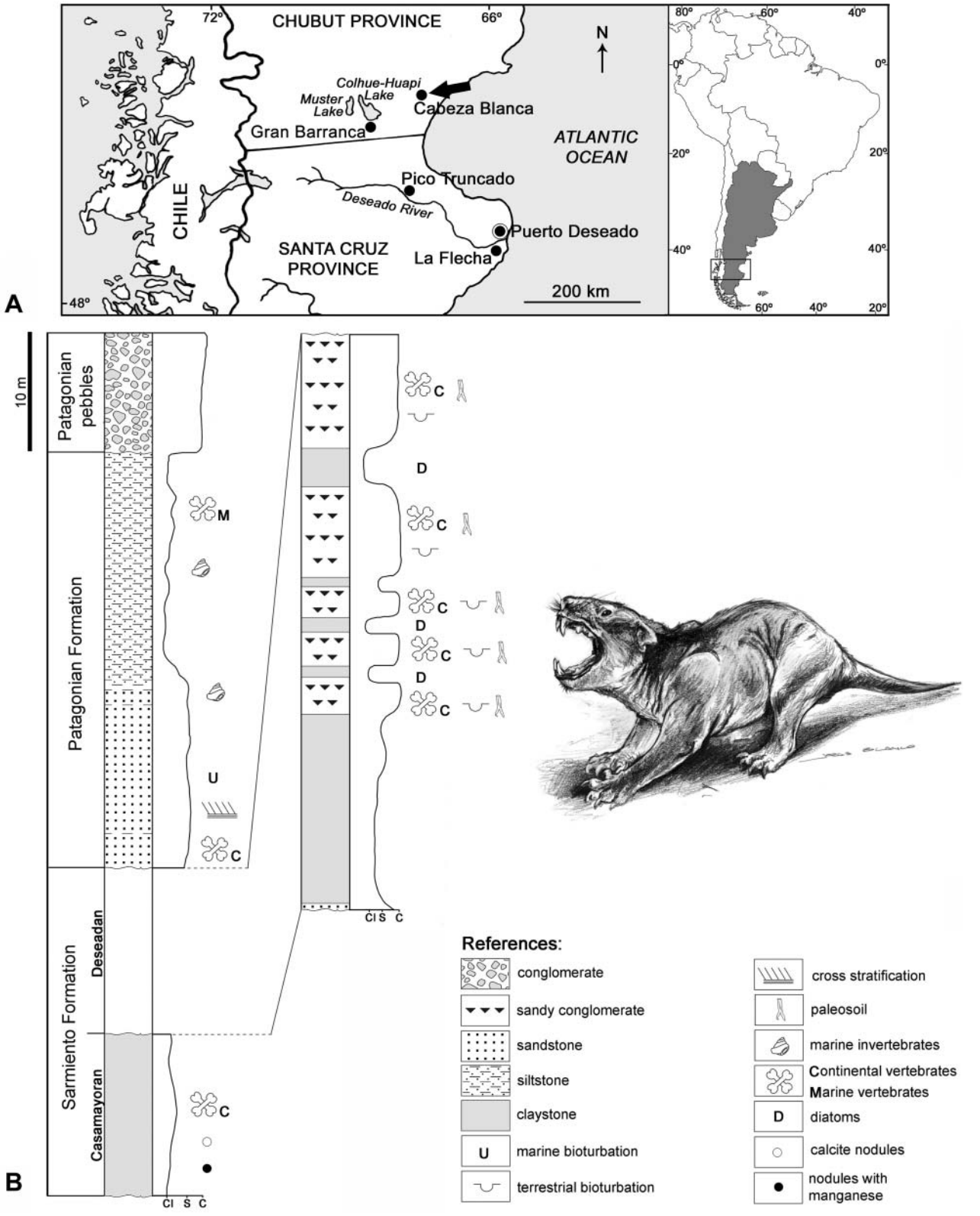

Figure 1. A, geographical location of specimens assigned to *Australohyaena antiqua*, Chubut and Santa Cruz Provinces, Argentina. The arrow indicates Cabeza Blanca where UNPSJB PV 113 was found; **B,** stratigraphical column exposed at Cabeza Blanca (based on Reguero & Escribano). Specimen UNPSJB PV 113 comes from the middle levels of the Sarmiento Formation exposed on the site (Late Oligocene; Deseadan age). The reconstruction of *A. antiqua* was created by Jorge Blanco.

-hyaena refers to the massive aspect of the skull, similar to living African hyaenids; also a common ending for large sized sparassodonts.

Australohyaena antiqua (Ameghino, 1894)
(Figs 2–6)

Diagnosis. Large Borhyaenidae characterized by a massive skull, short rostrum and wide palate. It differs from other borhyaenids (*Borhyaena* and *Arctodictis*) by having nasals extended beyond the level of the postorbital process, jugal extended more anterior than the lacrimal, postorbital process poorly developed and formed by the nasal and frontal, distinct preglenoid process of the squamosal, squamous part of the squamosal pierced by large foramina for emissary veins, dentary with coronoid process markedly inclined (anterior coronoid crest at 132° from the alveolar line); abrupt change in size between p1–p2 and p3; upper molars with broader stylar shelf on M3 and ectocingulum extending backwards up to the level of the metacone, M4 with three roots; lower molars with better developed talonid and distinct metaconid on m2–m4 separated from the talonid.

Referred specimens. MACN A 52-384, isolated left m3; FMNH P13633, crown of right lower canine; FMNH P13800, isolated right M3; UNPSJB PV 113, rostrum, basicranium, both dentaries, and dentition, except left i2, right i4 and right p1.

Occurrence. The type has no specific provenance. Marshall (1978) mentioned that MACN A 52-532 comes from 'capas de *Pyrotherium*', Chubut Province; although in the same year Patterson & Marshall (1978) tentatively considered the occurrence from La Flecha, Santa Cruz Province. These data disagree with those in a revised catalogue of the MACN, where the locality of Punta Nava is tentatively suggested. MACN A 52-384 is labelled 'Colhuapi *Pyroth*', which means the Deseadan horizon at Gran Barranca, Sarmiento Formation, Chubut Province (Patterson & Marshall 1978); FMNH P13633, La Flecha locality, Santa Cruz Province, Sarmiento Formation; FMNH P13800, Pico Truncado locality, Santa Cruz Province, Sarmiento Formation; UNPSJB PV 113, Cabeza Blanca locality, Chubut Province, Sarmiento Formation. Deseadan SALMA, Late Oligocene (Fig. 1A, B).

Description and comparisons. The skull is broken into two portions; one contains the rostrum and the immediately neighbouring postorbital and temporal regions, and the other includes the basicranium and posterior skull roof (Figs 2, 3). The skull of UNPSJB PV 113 has short rostrum and wide palate. The orbits are anterolaterally facing, suggesting the capability of stereoscopic vision. The postorbital width is wider than the basicranium (measured at the base of the zygomatic arches).

The nasal (Fig. 2A, B) is narrow at the anterior half, conspicuously widening at the level of the lacrimal. The anterior border does not overhang the narial fossae, as in other sparassodonts, and differs from other basal metatherians (e.g. *Deltatheridium*, *Peradectes*, *Andinodelphys* and *Mayulestes*) and living marsupials (*Didelphis*, *Monodelphys* and *Dromiciops*) (de Muizon 1998; Wible 2003; Babot 2005; Forasiepi 2009) in which the bone extends forwards. At the level of the contact with the maxilla and the lacrimal, the nasal has one large nutrient foramen at both sides of the skull. Specimens of *Callistoe* (PVL 4187), *Arminiheringia* (MACN A 10970) and *Borhyaena* (PU YPM 15701) have a small foramen in the mid-dorsal part of one nasal. *Borhyaena* (PU YPM 15120) has two foramina in the left nasal and one in the right (Sinclair 1906, lam. 43). Openings in the dorsal surface of the nasal for nerves and associated vasculature are frequent in mammals (e.g. Wible & Rougier 2000). The posterior border of the nasal projects behind the level of the postorbital process, which is even more posterior than in the sparassodonts compared. In dorsal view, the nasal–frontal suture is almost straight; the wedge of the frontal that other sparassodonts have is absent in *Australohyaena*.

The facial process of the premaxilla (Fig. 2A) is narrow and the posterodorsal process is very short, extending up to the level of the posterior border of the canine. The paracanine fossa is entirely contained in the premaxilla, as in other sparassodonts. A sharp edge closes the fossa dorsally. The narial platform is broad (Fig. 2B). The alveolar process of the premaxilla is straight with the alveoli of the upper incisors aligned (Fig. 2C). The palatal process of the premaxilla is short and the medial palatine process is slightly dorsally projected (i.e. it is not contained in the same horizontal plane as the palate), as in other borhyaenids. The incisive foramen is oval, mostly included in the premaxilla, and posteriorly bordered by the maxilla.

The facial process of the maxilla is broad and tall, with roughly semicircular shape (Fig. 2A). The infraorbital foramen is large and opens at the level of the posterior root of P3. The infraorbital canal is short and similar in length to other short-snout borhyaenids (e.g. *Borhyaena* and *Arctodictis*). In the left side of the maxilla, there is a small foramen below the infraorbital foramen. A short horizontal canal connects this small aperture with the infraorbital foramen which could carry an accessory division of the maxillary branch of the trigeminal nerve. Most sparassodonts lack extra openings of the infraorbital canal; accessory apertures were observed in *Arminiheringia*, *Callistoe*, and two specimens of *Borhyaena tuberata* (MACN 9341, YPM PU 15701). The dorsal border of the facial process of the maxilla is perforated by numerous, small nutrient foramina. The root of the canine defines a convex surface that almost reaches the dorsal border of the bone. *Australohyaena* has flaring cheeks, which are better seen in ventral view (Fig. 2C), in common with

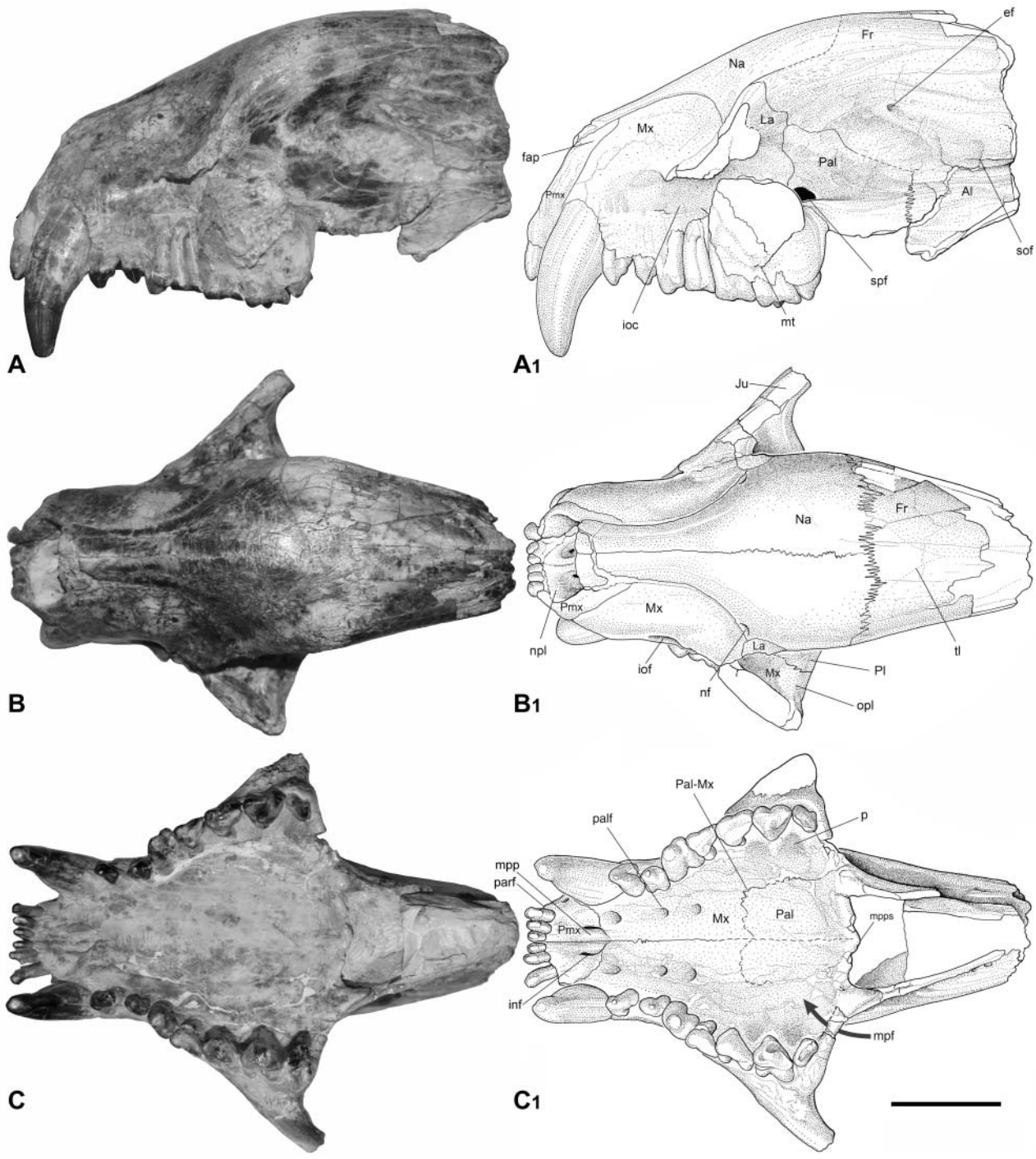

Figure 2. *Australohyaena antiqua*, UNPSJB PV 113, Late Oligocene, Deseadan, Cabeza Blanca, Chubut, Argentina; fragment of the snout in: **A,** lateral; **B,** dorsal; and **C,** ventral views. Abbreviations: Al, alisphenoid; ef, ethmoidal foramen; fap, facial process of premaxilla; Fr, frontal; iof, infraorbital foramen; ioc, infraorbital canal; inf, incisive foramen; Ju, jugal; La, lacrimal; mpf, minor palatine foramen; mpp, medial palatine process; mpps, medial postpalatine spine; mt, maxillary tuberosity; Mx, maxilla; Na, nasal; nf, nutrient foramen; npl, narial platform; opl, orbital platform; p, pit for reception of protoconid; Pal, palatine; palf, palatine foramen; parf, paracanine fossa; Pmx, premaxilla; spf, sphenopalatine foramen; tl, temporal line. Scale bar: 5 cm.

other sparassodonts (e.g. *Sipalocyon*, *Arminiheringia* and *Borhyaena*). The palatal process of the maxilla (Fig. 2C) is short and wide. The major palatine foramen is absent; several foramina disperse on the palatal surface and would carry branches of the major palatine nerve and artery, as probably occurred in other sparassodonts (Babot 2005; Forasiepi 2009). There are three major pairs of foramina: the first is the largest and is situated at the level of the posterior border of the canine, the second is at the level of P2, and the third is at the level of the anterior root of P3. The exact position and size of the apertures vary between the right and left maxilla. There is another foramen in the left palate at the level of the posterior root of M3. Additional small foramina are dispersed over the palatal surface. The minor palatine foramen is partially broken, but deduced from the bases it was small, with the ventral bridge formed by the palatine and the maxilla, again, common to most other sparassodonts (de Muizon 1998; Babot 2005; Forasiepi 2009). There is a deep dental pit between M3 and M4 that houses the protoconid of the m4 in occlusion. A shallow pit exists between M2 and M3. The orbital platform (Fig. 2B) is triangular, with shallow grooves and small alveolar foramina (Fig. 2B).

The zygomatic arch is broken on both sides of the skull (Fig. 2A, B), preserving the anterior base formed by the maxilla and the jugal (the latter present only in the left side of the skull) and a small portion of the posterior base formed by the squamosal. The suture between the maxilla and the jugal is oblique and at a shallower angle to *Borhyaena* and *Arctodictis* in which it is nearly vertical (Forasiepi 2009). The jugal extends more anteriorly than the lacrimal: when tracing a perpendicular line, the jugal extends up to the level of M2, whereas the lacrimal does up to the level of M3.

In ventral view (Fig. 2C), the horizontal process of the palatine exposes on the third posterior portion of the palate. It extends anteriorly up to the level of the anterior root of M2, describing an opened 'W', and posteriorly behind the posterior border of M4. The ventral border of the choana is thick and biconcave, with a blunt postpalatine spine. In common with other sparassodonts, the palatine torus, which is present in basal metatherians (*Mayulestes*, *Pucaldelphys* and *Andinodelphys*; de Muizon 1998, 1999) and living marsupials (*Monodelphys*, *Dromiciops* and *Dasyurus*; de Muizon 1999; Wible 2003; Forasiepi 2009), is absent in *Australohyaena*. There is a small contribution of the palatine to the medial wall of the orbit and floor of the infraorbital canal by means of the perpendicular process (Fig. 2A). The sphenopalatine foramen is oval and located at the joint between the floor and wall of the orbit. On the right palatine, posterior to the sphenopalatine foramen and at the level of its dorsal border, there is a small aperture that probably corresponds to a nutrient foramen.

The facial process of the lacrimal is crescent-shaped and almost restricted by the orbital rim. The lacrimal tubercle is damaged, but its base suggests that it was prominent, similar to other borhyaenids (Babot *et al.* 2002; Babot 2005; Forasiepi 2009). The lacrimal foramen is single and opens inside the orbit. The contribution of the lacrimal to the orbital wall is larger than in other borhyaenids (e.g. *Arctodictis*). The orbital surface is kidney-shaped with a frontal wedge interposed. In other sparassodonts, the posterior border of the lacrimal is mostly concave.

In dorsal view (Fig. 2B), the frontal is slightly convex. The postorbital process is blunt and poorly developed in comparison to other sparassodonts, and involves the nasal and frontal, unlike other sparassodonts, where it involves only the frontal (*Sipalocyon*, *Cladosictis*, *Prothylacynus*, *Callistoe*, *Arctodictis*). The temporal lines are short and restricted to the area near the midline of the skull. The two temporal lines join to form the sagittal crest, which is weak at its anterior base. In lateral view (Fig. 2A) the sphenorbital fissure is large and posteriorly bordered by the alisphenoid. The ethmoidal foramen is small, anterior and dorsal to the sphenorbital fissure. The orbitotemporal crest is weak and only evident in the anterodorsal neighbouring area of the sphenorbital fissure, running oblique towards the postorbital process. In other sparassodonts, the crest is sharper and the division between the orbit and the temporal fossa is more evident.

The fragment that contains the basicranium consists of part of the parietal and/or interparietal, alisphenoid, squamosal, basisphenoid, occipital bones, and a fragment of the right petrosal. In dorsal view (Fig. 3A) the skull roof is formed by one bone, which could be the parietal, the interparietal, or both. In some other sparassodonts (e.g. *Sipalocyon* and *Cladosictis*) these two bones are separated by a suture, but in other taxa (e.g. borhyaenids, *Callistoe*) only one bone is observed that could represent the fusion of the parietal with the interparietal (de Muizon 1999; Forasiepi 2009). This condition is found in several mammals (Koyabu *et al.* 2012). In UNPSJB PV 113, the entire bone surface has deep rugosities that suggest the attachment of a strong temporal musculature. Although the sagittal crest is broken at its base, the robust section of the remains is in accordance with well-developed temporal musculature.

The squamosal is partially preserved in UNPSJB PV 113. The squamous part is dorsally extended, reaching almost to the skull roof (Fig. 3A). There are two large foramina and an extra smaller one on the right side of the skull. These apertures are referred as emissary foramina, interpreted as associated with the venous drainage from the temporal fossa (Hiatt & Gartner 1987). Similar openings are present in *Paraborhyaena* and *Thylacosmilus* (Petter & Hoffstetter 1983; Babot 2005). There are, in addition, weak grooves that radiate from the foramina that probably are the impression of the soft tissues that these apertures conveyed. On the right side of the skull and

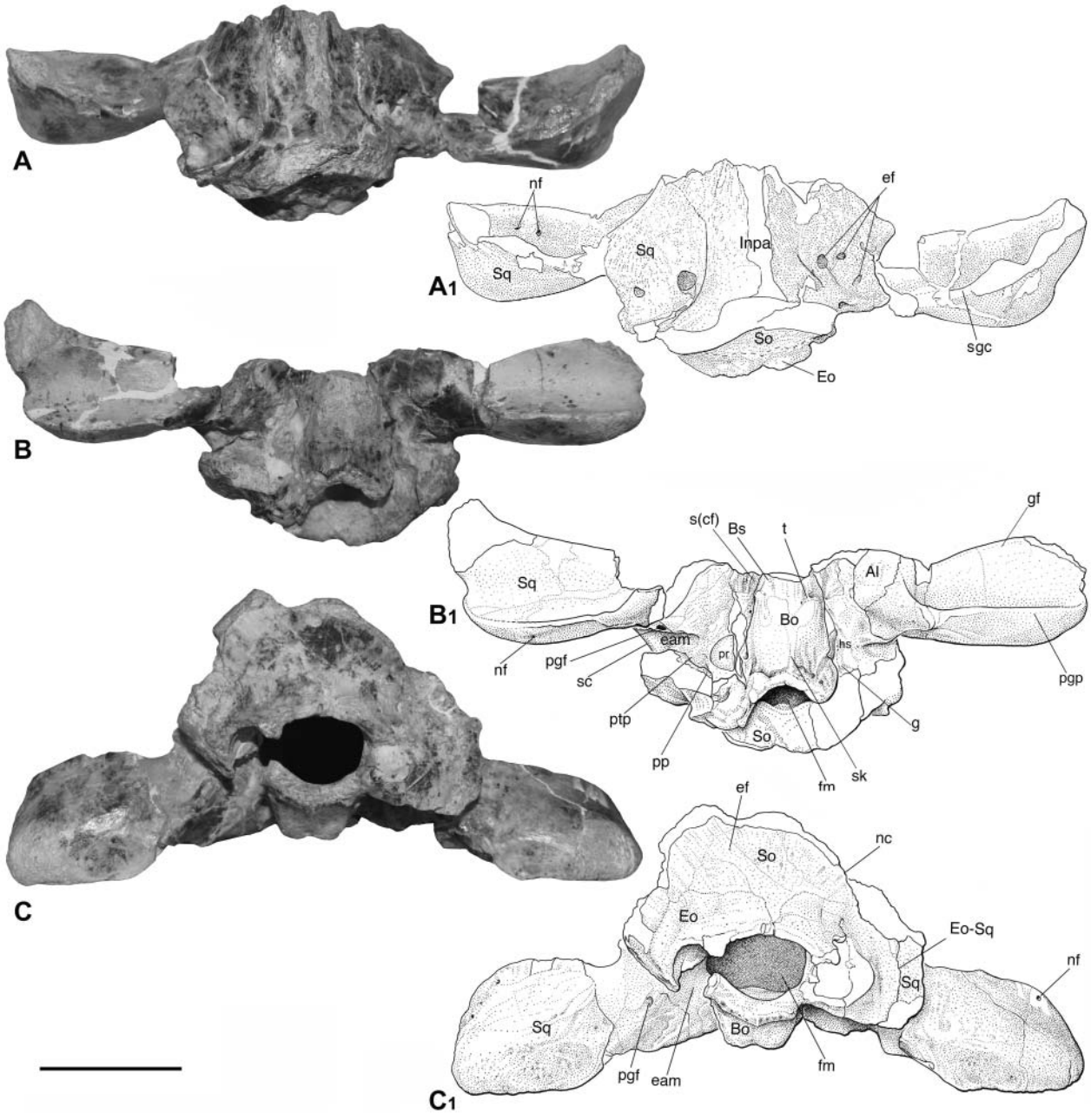

Figure 3. *Australohyaena antiqua*, UNPSJB PV 113, Late Oligocene, Deseadan, Cabeza Blanca, Chubut, Argentina; posterior portion of the skull in: **A,** dorsal; **B,** ventral (basicranium); and **C,** posterior views. Abbreviations: Al, alisphenoid; Bo, basioccipital; Bs, basisphenoid; eam, external auditory meatus; ef, emissary foramina; Eo, exoccipital; fm, foramen magnum; g, groove; gf, glenoid fossa; hs, hypotympanic sinus; Inpa, interparietal fused to parietal; nc, nuchal crest; nf, nutrient foramen; pgf, postglenoid foramen; pgp, postglenoid process; ptp, post-tympanic process of the squamosal; pp, paracondylar process; pr, promontorium of the petrosal; sc, suprameatal crest; s(cf), sulcus leading to the carotid foramen; sgc, supraglenoid crest; sk, sagittal keel; So, supraoccipital; Sq, squamosal; t, tubercles. Scale bar: 5 cm.

above the external auditory meatus (EAM), there is a small aperture posterolaterally oriented that may correspond to the suprameatal foramen. Its symmetrical condition could not be confirmed because of breakage in the left side. The suprameatal crest is blunt and connects the supraglenoid and nuchal crests.

The glenoid fossa (Fig. 2B) is wide (the width is twice its anteroposterior length) and formed mostly by the squamosal with no contribution from the alisphenoid, unlike living marsupials (de Muizon 1998, 1999). The jugal is not preserved but the broken surface suggests that it would contribute to the anterior border of the fossa as in other

sparassodonts. The glenoid fossa is limited by the preglenoid and postglenoid processes of the squamosal anteriorly and posteriorly, respectively. Dissimilar from other sparassodonts (e.g. *Borhyaena*, *Arctodictis*), the preglenoid process of the squamosal is tall, only slightly lower than the postglenoid process. The postglenoid process is half the length of its width, in common with other borhyaenids (e.g. *Cladosictis*, *Prothylacynus*, *Borhyaena*, *Fredszalaya* and *Callistoe*). In dorsal view and dorsal to the glenoid fossa, the surface of the squamosal has three principal depressions that suggest the attachment of the strong temporal musculature, as in *Callistoe* and *Paraborhyaena* (Babot 2005). On the left side of the skull, there are two small apertures that communicate with each other by a superficial canal and probably are accessory apertures related to the venous drainage of the temporal musculature. In posterior view (Fig. 3C), a small foramen opens at the lateral angle of the postglenoid process. Similar openings were observed in the squamosal of living marsupials (unnamed foramen in Wible 2003).

The EAM is deep, wide, and enclosed between the postglenoid and post-tympanic processes. The anterior wall of the meatus is pierced by a large postglenoid foramen, located at the level of the medial border of the glenoid fossa. This position is common in most sparassodonts with the exception of some taxa (e.g. *Lycopsis* and *Hondadelphys*) in which it occupies a more lateral position. The post-tympanic process of the squamosal is robust and rises together with the paracondylar process of the exoccipital.

The hypotympanic sinus is a broad cavity excavated in the alisphenoid, squamosal and petrosal (Fig. 3B). The petrosal position in the basicranium is almost vertical, with the main axis only slightly inclined in the anteroventral–posterodorsal direction. This is also the condition in *Paraborhyaena* and *Callistoe* (Petter & Hoffstetter 1983; de Muizon 1999; Babot *et al.* 2002). The general aspect of the petrosal is elongated, more in common with the specimen AMNH 29591 referred as cf. *Pharsophorus* sp. than with *Borhyaena* and *Arctodictis*, which are shorter and more compact. The promontorium is bulbous, even more than in cf. *Pharsophorus*. There is a low crest-like rostral tympanic process pointing forward, similar to all known sparassodonts, instead of the vertical process described for living didelphids (Wible 2003; Ladevèze & de Muizon 2010). In cerebellar view, the internal acoustic meatus is slightly more oval than in cf. *Pharsophorus*, and the subarcuate fossa is slightly shallower than in the aforementioned specimen.

A small portion of the alisphenoid contributing to the ear region is conserved in the specimen UNPSJB PV 113. The suture with the squamosal is nearly vertically and slightly medially oblique to the hypotympanic sinus. The foramen ovale is represented by a notch at the anterior border of the hypotympanic sinus (the posterior border is incomplete), described in some large size borhyaenoids (e.g. *Fredszalaya*, *Callistoe*, *Borhyaena* and *Arctodictis*). There is no evidence of an alisphenoid tympanic process, neither of the transverse foramen, assuming that both structures were absent in *Australohyaena*, again similar to some borhyaenoids. The paracondylar process of the exoccipital is slightly anteriorly inclined. There is an accessory sinus developed directly posterior to the petrosal (Fig. 3C).

The anterior border of the exoccipital, medial to the paracondylar process, has a small notch through which the jugular vein and accompanying nerves and vessels would pass. The jugular foramen primarily develops between the exoccipital and the petrosal (Wible 2003). According to the position of the petrosal, the primary jugular foramen would open deep inside the basicranium. The notch seen in ventral view is the outer expression of the aperture, similar to *Arctodictis*, *Borhyaena* (Forasiepi 2009) and *Callistoe* (Babot 2005).

The basioccipital is nearly rhomboidal (Fig. 3B). There is a low sagittal keel which separates two shallow fossae, and anteriorly a pair of tubercles, probably related to the attachment of the muscles rectus capitis ventralis and longus capitis (Evans & Christensen 1979). In lateral view, the borders of the basioccipital are thick and have a deep sulcus that runs almost horizontally. The sulcus leads to the carotid foramen (e.g. *Callistoe* and *Borhyaena*), but this foramen is not preserved in UNPSJB PV 113.

The occiput (Fig. 3C) is formed by the supraoccipital, exoccipital and squamosal. The mastoid portion of the petrosal is excluded from the occiput, in common with other sparassodonts. There are several small foramina dispersed over the posterior surface of the supraoccipital, with the largest located close to the sagittal plane, which probably carried emissary veins, connecting with the intracranial sinuses. The foramen magnum is bordered by the exoccipital in posterior view and by the basioccipital in ventral view, as in other sparassodonts (e.g. *Prothylacynus*, *Paraborhyaena* and *Callistoe*). The nuchal crest is damaged, but the preserved base suggests that it was thick and robust. The occipital condyles in UNPSJB PV 113 are not preserved, nor are the foramina associated with them (i.e. hypoglossal foramina).

Endocranium. The contribution of the parietal–interparietal bones to the posterior skull roof is significant in the internal part of the skull. The lateral walls of the endocranium are formed by the squamosal, exoccipital, and a small contribution from the petrosal. The floor is formed by the basioccipital. There is a deep cavity on the posterior sagittal plane, where the vermis of the cerebellum would be housed, similar to *Arctodictis*, *Borhyaena* and *Paraborhyaena* (Quiroga 1978; Petter & Hoffstetter 1983; Forasiepi 2009). Lateral to this depression there is a smaller and shallower concavity on each side of the skull, where the cerebellar hemispheres were housed. The

difference in size between the vermis and the cerebellar hemispheres is clearer in UNPSJB PV 113 than in *Borhyaena*, *Arctodictis*, and apparently *Paraborhyaena*. In *Borhyaena* these depressions are similar in size (Quiroga 1978; Forasiepi 2009). Judging by the size of these fossae and the fossa subarcuata, the cerebellum of *Australohyaena* seems to have been larger than the crown Marsupialia, in common with some basal metatherians (i.e. *Pucaldelphys*) (Macrini *et al*. 2007). A V-shaped groove emerges from the front of the depression for the vermis that would correspond to the most posterior impression of the sagittal sinus and its division into the transverse sinuses. In the right lateral side of the skull, the subsquamosal foramen opens close to the ventral end of the transverse sinus and close to the anterior border of the petrosal.

Dentary. The symphysis extends to the level of the posterior root of the p3 (Fig. 4). In anterior view (Fig. 5A), a small fissure between both dentaries suggests that the fusion along the symphysis is incomplete, similar to other borhyaenids (e.g. *Arctodictis sinclairi* and *Borhyaena tuberata*). For other sparassodonts the suture is either entirely fused (e.g. *Arctodictis munizi*, *Callistoe* and *Paraborhyaena*) or the two dentaries are joined by ligaments (e.g. *Patene*, *Acyon* and *Cladosictis*). The horizontal process or body is deep, with nearly the same height all along its length (Fig. 4A). A subtle difference in height is between the lateral and the medial side of the dentary, with the medial side being the tallest. The ventral border is straight, curving upwards gradually at the anterior and posterior ends. There are five mental foramina in the right dentary. A small portion is broken in the left dentary at the level of the canine, possibly concealing the presence of a fifth foramen to the four visible on this side. The mental foramina have subtle differences in size and position. The most anterior foramen in the right dentary is the smallest and is situated at the level of the anterior border of the canine. The second foramen (the first that is clearly paired) is the largest and is located at the level of the

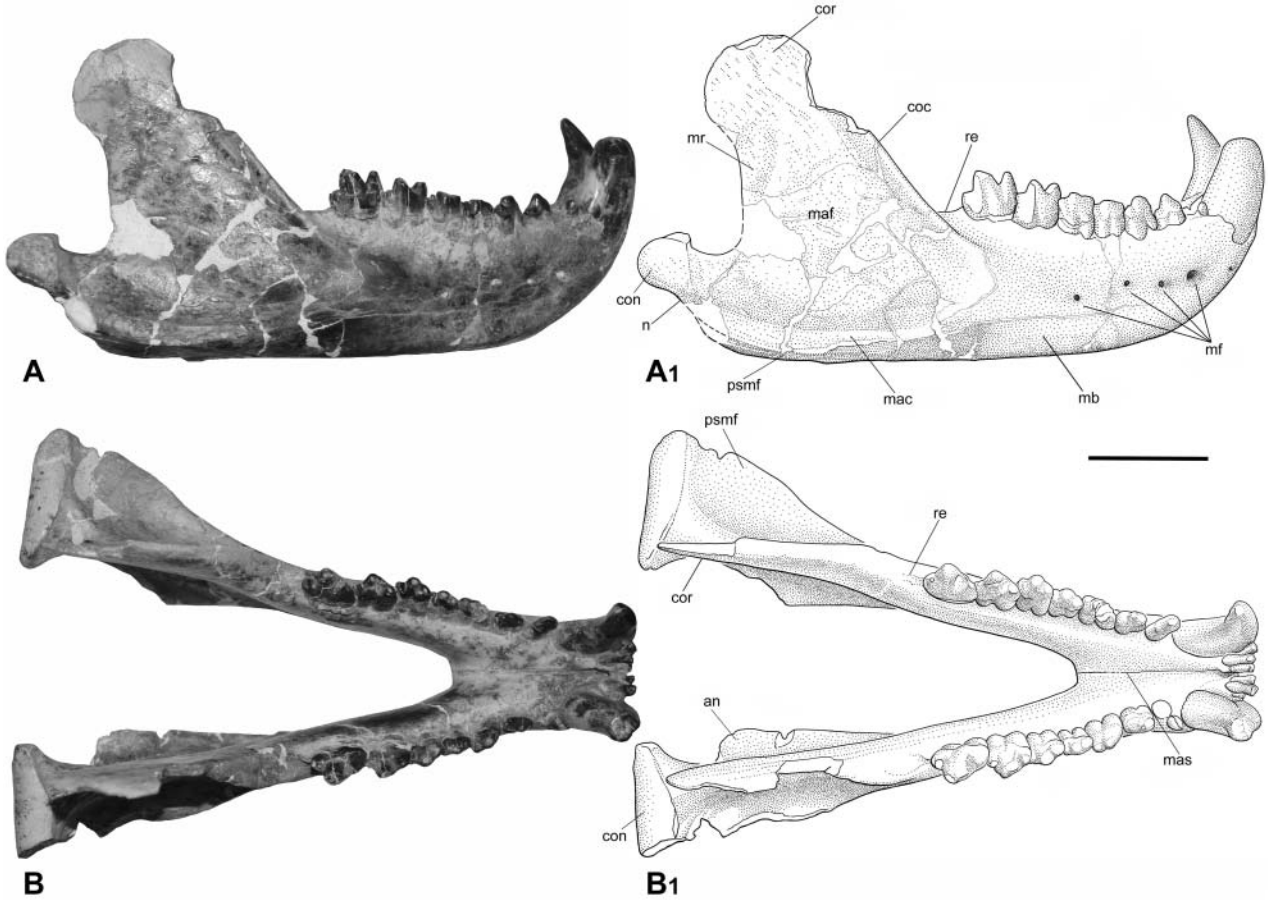

Figure 4. *Australohyaena antiqua*, UNPSJB PV 113, Late Oligocene, Deseadan, Cabeza Blanca, Chubut, Argentina; mandible in: **A,** lateral and **B,** dorsal views. Abbreviations: an, angular process; coc, coronoid crest; con, condylar process; cor, coronoid process; mac, masseteric crest; maf, masseteric fossa; mas, mandibular symphysis; mb, mandibular body; mf, mental foramina; n, neck; psmf, posterior shelf of the masseteric fossa; mr, mandibular ramus; re, retromolar space. White areas represent damage zones of the bones. Scale bar: 5 cm.

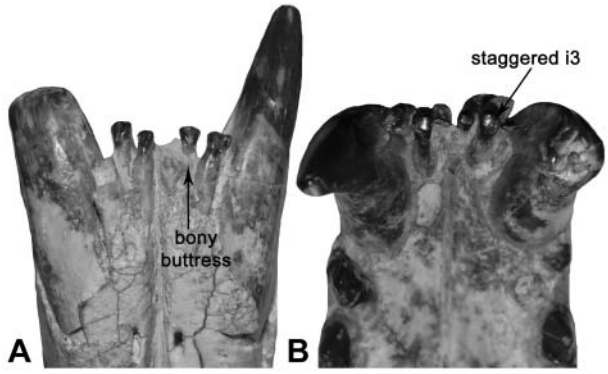

Figure 5. Detail of the mandible of *Australohyaena antiqua*, UNPSJB PV 113 with the incisor row in: **A,** mesial and **B,** occlusal views, indicating the bony buttress and the staggered i3.

anterior root of p2. The second pair of mental foramina is slightly smaller and almost similar to the remaining openings, and is located at the level of the posterior root of p2 in the left dentary and at the junction of p2−p3 on the right side. The third pair is located at the junction of p3−m1, and the fourth pair is below the m2. In addition, in anterior view, there are two pairs of other foramina, symmetrically located. One pair is set close to the alveolar border of the incisors (Fig. 5A), and the second pair set more ventral, in the same vertical line as the first pair. The retromolar space is nearly as long as the m1. The coronoid process is high, inclined posteriorly, even more than in other large sized sparassodonts (e.g. *Arctodictis*, *Borhyaena* and *Thylacosmilus*). The masseteric fossa is deep and delimited by protruding coronoid and masseteric crests. The condyle is cylindrical and is located below the level of the alveolar border, as in other sparassodonts. The neck distinguishes as the constriction below the condyle. The angular process projects ventromedially and forms a rough triangular shelf (Fig. 4B), which corresponds to the 'intermediate' state described by Sánchez-Villagra & Smith (1997) and characterizes large metatherians, including sparassodonts. The mandibular foramen is large and opens at the middle of the anteroposterior length of the coronoid process.

Dentition. The dental formula is 3/3; 1/1; 3/3; 4/4. The three upper and three lower incisors in *Australohyaena* are hypothesized to be homologous to I2−4/i2−4 of other metatherians (Forasiepi 2009). The upper incisors are crowded and set in a straight line. This condition is also present in most sparassodonts (e.g. *Cladosictis*, *Prothylacynus*, *Lycopsis*, *Borhyaena* and *Arctodictis*). The incisors increase in size to I4. The I4 is styliform and slightly laterally curved. It consists of a main cusp laterally followed by a blunt cingulum. The roots of all incisors are stout, notably in the I4, which is bulbous and set outside the alveolus.

The upper canine is robust and oval in cross section. The distribution of the enamel in the crown is irregular, covering more the lateral than the medial surface of the tooth. The root is surrounded by longitudinal grooves, mostly distributed on the labial surface. In the lingual side, there is one principal groove close to the mesial border of the tooth, which is deeper than the others. The presence of striations and grooves in the canines is common in large sparassodonts (e.g. *Arctodictis*, *Borhyaena*, *Callistoe*, *Paraborhyaena* and *Proborhyaena*). A breakage in the left side of the maxilla reveals that the canine is deeply inserted in its alveolus and probably reaches the dorsal border of the maxilla, as suggested by the convex surface defined on the maxilla.

The upper premolars are robust with bulbous roots exposed from their alveoli (Fig. 6A). The P1 is slightly smaller than the P2, and both are conspicuously smaller than the P3. The P1 is set oblique in the maxilla; the P2 is parallel to the anteroposterior axis of the palate, and the P3 set oblique but opposite to the first premolar. All premolars consist of a main cusp followed by a distal cingulum or heel. The P1−P2 have a short and weakly defined mesiolingual cingulum. The principal cusp is asymmetrical in the P1 and symmetrical in the P2−P3. There is a distal cusp in all premolars, larger in P3. The P3 is the most robust and the largest premolar. The morphology and the robustness of the P3 of *Australohyaena* resemble that of *Borhyaena* and *Arctodictis* more than any other sparassodont (Marshall 1978). The upper molars increase in size from the M1 to M3, with M4 being the smallest (Fig. 6A). All molars have three roots, including the M4. The crowns have strong wear facets obscuring their morphology, in particular in the M1−M2. In the M2, there is a narrow stylar shelf and an ectocingulum that extends backwards up to the level of the metacone. This last feature is also present in other sparassodonts such as *Borhyaena*, *Arctodictis*, *Callistoe* and *Proborhyaena*. In the M3, the metacone is the dominant cusp and occupies nearly a central position in the tooth. The paracone is coalescent with the metacone (there is no centrocrista). The protocone is very small and occupies a basal position in the crown. The stylar shelf is broad and has a similar width at the mesial and the distal part of the tooth. The ectocingulum is long, extending up to the level of the metacone. The ectoflexus is very shallow. The postmetacrista is twice longer than the preparacrista. The M4 has a tall paracone and a small metacone that is coalescent with the paracone. Other few sparassodonts (*Patene*, *Hondadelphys* and *Sallacyon*) exhibit a small metacone. The protocone is even smaller than in previous molars. The preparacrista is longer than in the M3 and the postmetacrista is absent. There is no stylar shelf.

The three lower incisors are tightly packed between the canines and arranged in a straight line, in the anterior part of the dentaries (Fig. 5). All the elements are roughly

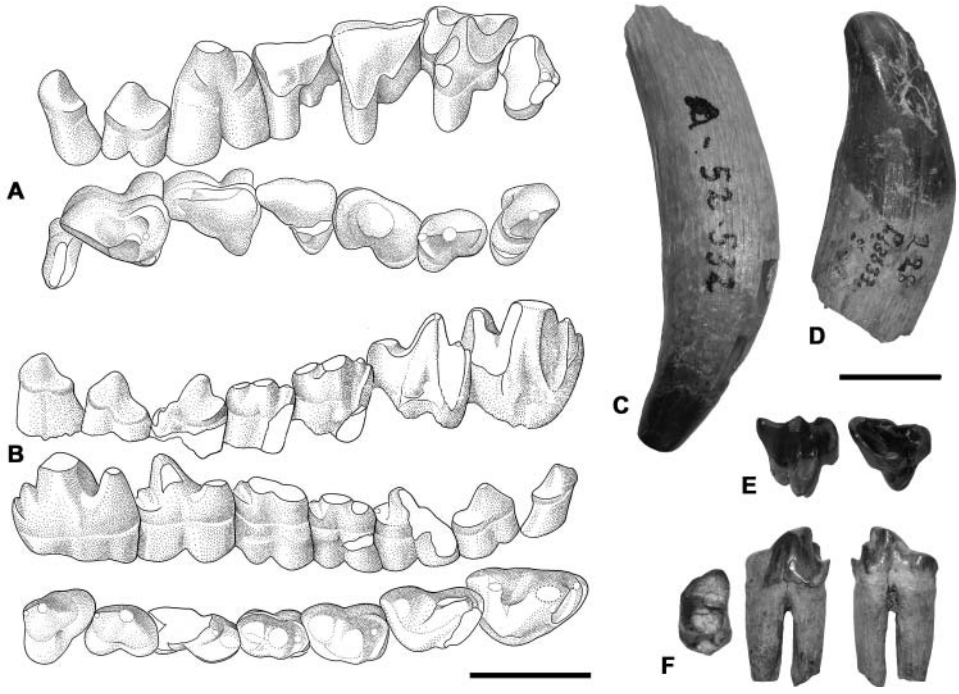

Figure 6. Dentition of *Australohyaena antiqua*. **A, B,** UNPSJB PV 113; **A,** left and right upper postcanines in lingual and occlusal views; **B,** left lower postcanines in labial, lingual and occlusal views; white areas represent worn zones of the teeth; **C,** holotype, MACN A 52-532, a nearly complete isolated right upper canine; **D,** FMNH P13633, right lower canine; **E,** FMNH P13800, isolated right M3 in lingual and occlusal views; **F,** MACN A 52-384, isolated left m3 in occlusal, labial and lingual views. Scale bar: 2 cm.

similar in size, with the i2 the smallest. In anterior view, the crown is triangular and narrower at the base. The i3 is staggered, in common with almost all other metatherians (Hershkovitz 1982, 1995), with a bony buttress (Fig. 5).

The lower canines are robust and oval in section with a bulbous root. The distribution of the enamel is also irregular, following the pattern of the upper canine. The canine is almost vertical and resembles many other borhyaenids, unlike *Arminiheringia* in which it is procumbent (Simpson 1948; Babot *et al*. 2002). The root has numerous vertical grooves, similar to the upper canine, with the deepest being in the lingual view.

The postcanine row is set slightly laterally oblique, meaning that when the jaw is seen in dorsal view, the teeth are leaning labially (Fig. 4B). The premolars are similar in robustness to the upper premolars and similarly oriented with the p1 oblique, the p2 parallel to the dentary axis, and the p3 oblique but opposite to the p1 (Fig. 6B). The p1 is slightly smaller than the p2, and the p3 is the largest. The difference in size between the p1−p2 and the p3 is more evident in the upper premolars. This change in size is more gradual in *Borhyaena* and *Arctodictis*. The crowns of premolars consist of a principal cusp followed by a large distal cingulum or heel. The principal cusp is asymmetrical in the p1−p2 and symmetrical in the p3. There is a cusp associated to the distal heel in all premolars that is large and bulbous in the p3. In lateral view, the p3 is slightly obliquely, distally inclined. This trait was classically considered a diagnostic feature of the genus *Pharsophorus* (Marshall 1978), although it is also present in *Plesiofelis*, *Borhyaena macrodonta* and *Arctodictis sinclairi*. The lower molars increase rapidly in size from the m1 to the m4 and are disposed slightly imbricately between each other (Fig. 6B). The roots are strong and parallel, exposed outside their alveoli. The molars consist of a tall protoconid followed by a paraconid mesially and a small distal cusp (hypoconid in m1 and metaconid in m2−m4; see Discussion). In the m1, the three cusps are aligned, whereas in the posterior elements, the three cusps form an angle that closes towards the m4. The paraconid is lower than the protoconid and this difference in height increases to the back. The precingulid is small in all premolars. The hypoconulid notch is shallow in the m1 and becomes deeper towards the m4. The talonid is vestigial. The hypoconulid is small and occupies a median position. The entocristid is short. The postcingulid is wide, extending more over the labial than over the lingual side of the tooth. This condition is very similar to that seen in borhyaenids such as *Borhyaena* and *Arctodictis*.

Discussion

Systematics

Taxonomy. Ameghino in 1894 (p. 655) made a provisional assignation of an isolated canine (the holotype,

MACN A 52-532; Fig. 6C) to the species ?*Borhyaena antiqua*. This material was in a faunistic association normally not connected to the species of *Borhyaena*, raising uncertainties despite strong similarities with the canine of *Borhyaena.* Later, Ameghino (1897) recognized the genus *Proborhyaena* and proposed the combination *P. antiqua* for that isolated piece.

In 1978, Marshall tentatively added into the hypodigm of *antiqua* the specimens FMNH 13366, a lower canine; FMNH 13800, an isolated M3; and MACN A 52-384, an isolated m3 (Fig. 6D–F). At the same time, Marshall suggested that the species was not *Proborhyaena* but a borhyaenid, probably *Pharsophorus*, combining the name*Pharsophorus*(?) *antiquus*.

The lower canine FMNH 13633 (Fig. 6D) has a deep vertical medial sulcus and extra shallower grooves at the bases, as in UNPSJB PV 113. The M3 FMNH 13800 (Fig. 6E) has the same size as the M3 of UNPSJB PV 113 and the crown is less worn. The stylar shelf is wide as in UNPSJB PV 113. The lingual margin has a long ectocingulum and a discontinuous crest with tiny cusps. The protocone is small and there are sharp parallel crests descending from the paracone and metacone to the protocone. Those features are present in UNPSJB PV 113 but obscured by wear. The m3 MACN A 52-384 (Fig. 6F) is slightly smaller than the m3 of UNPSJB PV 113. Both have a similar morphology, differing in the position of the metaconid (more lingual in MACN A 52-384) and in the morphology of the talonid (larger and more protruded in MACN A 52-384). We consider that these differences are intraspecific variation. Considering UNPSJB PV 113, we support the view of Marshall (1978) in recognizing the specimens FMNH 13366, FMNH 13800 and MACN A 52-384 as part of the hypodigm of the species initially described by Ameghino (1894) and here determined as *Australohyaena antiqua*.

Phylogeny. A cladistic analysis was performed to test the phylogenetic position of *Australohyaena antiqua* within Sparassodonta. The data matrix is based on Forasiepi (2009) and includes the modifications and additions recently proposed by Engelman & Croft (2014). New changes in the scoring were included and are indicated in the Supplemental Material.

The matrix has 307 morphological characters (107 cranial, 80 dental and 120 postcranial characters) that were scored for 19 sparassodonts and 20 species in the outgroup, including representatives of the crown group Marsupialia and stem marsupials (Supplemental Material). Forty-nine characters describing a logic sequence were ordered following Engelman & Croft (2014).

The data matrix was analysed using maximum parsimony (MP) with equally weighted characters and under implied weighted characters with the computer program TNT 1.1 (Goloboff *et al*. 2008a, b). The implied weight procedure uses evidence on homoplasy to estimate character reliability. The trees are constructed based on maximum reliable characters and have a better total fit (Goloboff 1993; Goloboff *et al*. 2008a).

Thylacinus cynocephalus was excluded because this taxon was grouped in all the trees with the Sparassodonta (see also Forasiepi 2009 and Engelman & Croft 2014). *Thylacinus* is a Dasyuromorphia as supported by molecular analysis (e.g. Thomas *et al*. 1989; Krajewski *et al*. 1992, 1997) and the anatomy of the tarsal bones (Szalay 1982, 1994). The inclusion of *Thylacinus* within sparassodonts in our tree is based on homoplasies.

The equally weighted MP analysis was conducted by searching Wagner trees with 500 random addition sequences, followed by tree bisection reconnection (TBR), and saving 10 trees per round. The analysis resulted in five most parsimonious trees of 1022 steps (consistency index [CI] = 0.373, retention index [RI] = 0.676). The strict consensus and Bremer index of the nodes are shown in Fig. 7A. The list of synapomorphies is in the Supplemental Material. The consensus tree has two major divisions for the Sparassodonta, the Hathliacynidae and Borhyaenoidea, and stem taxa. The internal arrangement of hathliacynids is different among the five resulting trees and this is shown as a polytomy in the consensus. In addition, no agreement is found by comparing the results of different authors (e.g. de Muizon 1999; Babot *et al.* 2002; Babot 2005; Forasiepi *et al.* 2006; Forasiepi 2009; Engelman & Croft 2014), suggesting that the hathliacynid relationships deserves a particular analysis. Borhyaenidae (including *Australohyaena antiqua*) and Thylacosmilidae are represented in our analysis as monophyletic groups (Fig. 7A). Conversely, Proborhyanidae is not shown as monophyletic, with *Callistoe* and *Paraborhyaena* placed as successive stem taxa of Thylacosmilidae. The recognition of Proborhyaenidae as a monophyletic group is still a controversial issue. Some recent studies have recorded them as monophyletic (e.g. Babot *et al*. 2002; Engelman & Croft 2014), although the most exhaustive analysis that included several species of this group recorded them as paraphyletic (Babot 2005). *Pharsophorus lacerans* is placed as the sister taxon of the monophyletic group formed by Borhyaenidae, Thylacosmilidae, and the paraphyletic Proborhyaenidae.

The analysis under implied weights (K = 3) provided one tree with fit = 110.16 (Fig. 7B). The principal difference in the sparassodont relationships comparing the trees under equal and implied weighted characters is the arrangement and position of proborhyaenids. Under implied weights, *Callistoe* and *Paraborhyaena* are sister taxa, supporting the monophyly of Proborhyaenidae. Proborhyaenidae is placed as the sister taxon of Borhyaenidae and Thylacosmilidae, similar to the arrangement obtained by Engelman & Croft (2014) with MP under equal weighted characters. By constraining this arrangement of

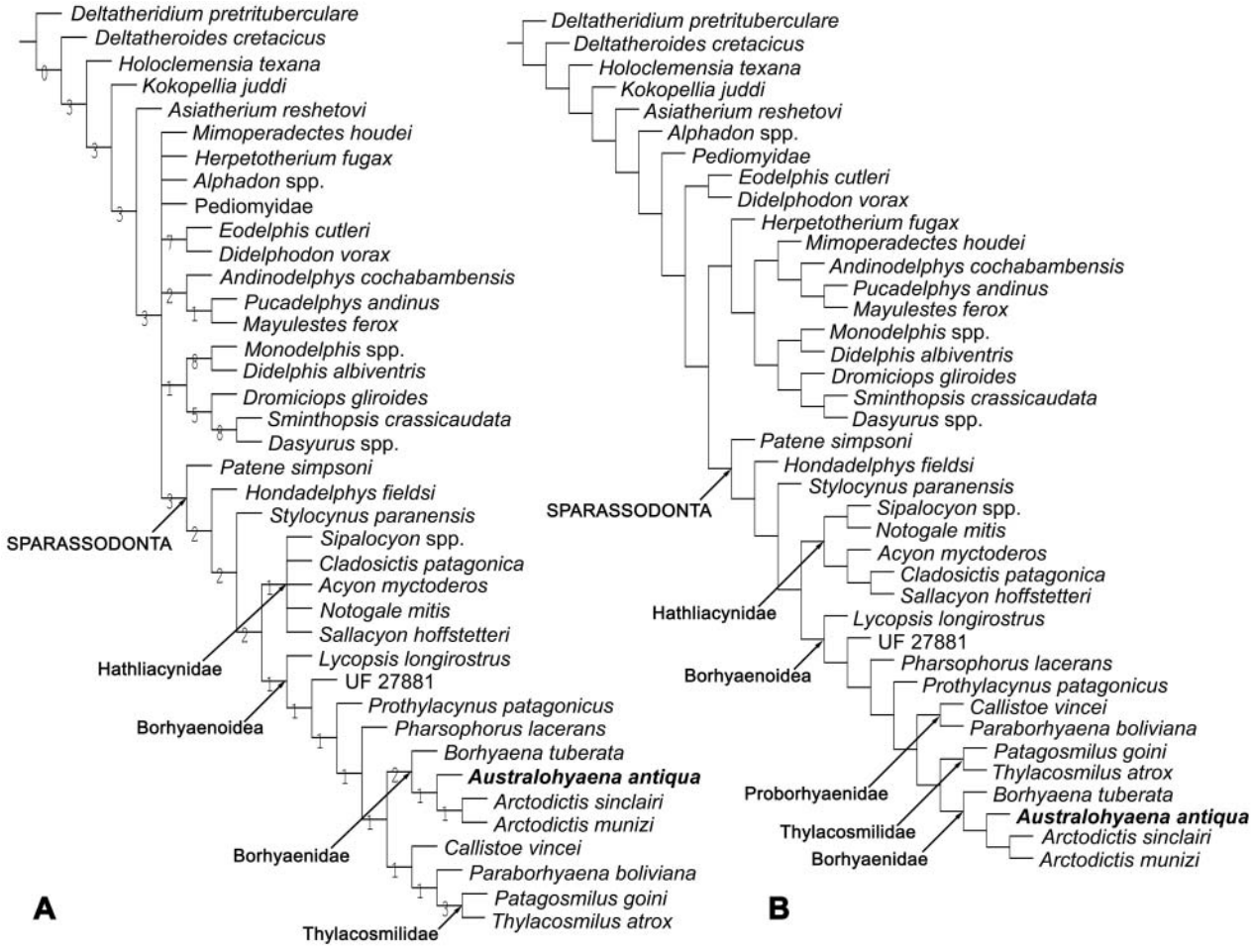

Figure 7. Phylogenetic trees. **A,** strict consensus cladogram of five trees obtained with equally weighted characters (1022 steps, CI = 0.373, RI = 0.676); numbers at nodes indicate Bremer support values; **B,** single tree obtained with implied weighted characters (K3; fit = 110.16).

the groups in our five MP trees with equal weighted characters, only a single extra step (length 1023) is required to obtain Proborhyaenidae as monophyletic and basal to Borhyaenidae and Thylacosmilidae. As previously observed, the monophyletic nature of the Proborhyaenidae requires clarification in future analyses.

Because the homologies of the lower molar talonid cusps within Borhyaenidae has been subject of different interpretations (Marshall 1978; Goin *et al*. 2007; Forasiepi 2009), a second analysis was performed re-coding as uncertain (?) the features related to the entoconid, hypoconulid, hypoconid, metaconid and associated crests for the m1−m4 in Borhyaenidae. The characters involved in the re-coding were 169, 176−180, 182, 183 and 184 in *Borhyaena tuberata*, *Arctodictis munizi*, *Arctodictis sinclairi* and *Australohyaena antiqua*. The MP analysis under equally weighted characters resulted in five most parsimonious trees of 1021 steps (CI = 0.373; RI = 0.674). These trees have the same topologies as those originally obtained with the characters coded for Borhyaenidae. The strict consensus has the same topology, except Borhyaenidae has a support of 1 instead of 2 as in the original results (Supplemental Material). In addition, the analysis under implied weights (K = 3) provided one tree with fit = 110.01 that has the same topology as the tree obtained in the original analysis. The re-coding of those lower molar characters as uncertain has not influenced the topology of the resultant tree. Our primary homology can be supported.

Considering the analyses, the metaconid in the Sparassodonta was lost in the common ancestor of hathliacynids and borhyaenoids. This cusp is registered again in the m2−m4 in *Pharsophorus lacerans* and Borhyaenidae (character length: 3). In *Arctodictis* and some specimens of *Borhyaena* the m4 metaconid is lost (see Discussion). In addition, sparassodonts have a small or non-existence entoconid, a reduction of the talonid dimension and associated structures. This is particularly stressed in borhyaenids, thylacosmilids and proborhyaenids. The alternative view of considering the posterior trigonid cusp of

borhyaenids homologous to an enlarged entoconid seems unlikely in the context of their molar morphology (see Discussion).

In all the analyses, *Australohyaena antiqua* was grouped with *Borhyaena* and *Arctodictis* within Borhyaenidae. The monophyletic Borhyaenidae was recorded in all the phylogenetic trees. *Australohyaena antiqua* is clearly separated from *Pharsophorus lacerans* and the latter is located basal to borhyaenids, thylacosmilids and proborhyaenids (Fig. 7A, B). Our interpretation of the taxonomy, i.e. the recognition of a new genus for *antiqua* to distinguish this taxon from *Pharsophorus lacerans* with different generic names, is based on the phylogenetic analysis. Finally, in all our trees UF 27881, recently described by Engelman & Croft (2014), appears as a Borhyaenoidea and this arrangement differs from the analysis recently presented which locates this taxon as a plesion Sparassodonta. The support we obtained for the node that includes UF 27881 and other parts of the tree is low (Fig. 7A). Alternative arrangements are possible with recoding characters and adding new taxa.

Palaeoecology

In living mammals, the niche of carnivory is subdivided into three categories (hypercarnivores, mesocarnivores and hypocarnivores) according to the proportion of meat included in the diet (Van Valkenburgh 1988, 1989).

The hypercarnivorous diet consists of more than 70% of vertebrate material (Van Valkenburgh 1999) and taxa are arranged in three ecomorphs. The cat-like type has a short snout, larger and vertical incisors, elongated and laterally compressed canines, shearing premolars, carnassial molars without talonids and reduced post-carnassial dentition (Van Valkenburgh 2007). The jaw is deeper at the level of the carnassials. The hyaena-like type or bone-cracker has a short snout, robust sagittal crest, and vaulted skull (Werdelin 1989). The premolars are robust, conical, and located where the bite force is maximal (Werdelin 1987, 1989). As a consequence, the jaw has a similar depth below the premolars and carnassials (Werdelin 1987). The wolf-like type or bone-crusher shows a long and wide snout, narrow premolars, and talonids in the carnassials with one cusp which is blade-like, forming a 'trenchant-heel' (Van Valkenburgh 2007). Contrary to the highly specialized hypercarnivores, the mesocarnivores and hypocarnivores have more uniform morphology. The mesocarnivore diet consists of between 50% and 70% of vertebrate material (Van Valkenburgh 1999). The snout is larger than in hypercarnivores, the jaws are shallower, and the carnassial lower molars have talonids with two cusps (Van Valkenburgh 1999). Low grinding activity occurs in the carnassials, giving great versatility in the item consumption. Hypocarnivores, or omnivores, have a diet that consists of about 30% of vertebrate material and the remainder is mainly composed of invertebrates and fruits (Van Valkenburgh 1999, 2007). Their skull and dentition is more generalized. They have well-developed post carnassial molars with broad and cuspated talonids, and the trigonids have shorter and blunt crests (Van Valkenburgh 2007). The palaeobiological aspects (body mass and feeding preferences) of *Australohyaena antiqua* are examined in the light of these definitions using morphometric variables.

Body mass. Equations based on tooth measurements (Gordon 2003) and craniodental measurements (Myers 2001) were used to estimate the body mass of UNPSJB PV 113 (Table 1). For dental measurements, the best predictor variables are the length of the second upper molar (M2L) and the length of the third lower molar (m3L) (Zimicz 2012). The craniodental variables selected are: the lower and upper molar occlusal row length (LOMRL and UOMRL); the total jaw length (TJL), measured from the base of the first incisor to the posterior border of the dentary (i.e. condyle); and the posterior jaw length (PJL), measured from the posterior border of m4 to the posterior border of the condyle.

The estimation of 67 kg based on m3L for the body mass of UNPSJB PV 113 is selected because it presents low values of %PE (12%) and good adjusted R2 (0.95). The lowest value of %PE (7%) corresponds to the estimation based on M2L (44 kg). This value is probably an underestimate taking into account that the skull length of UNPSJB PV 113 is 50% longer than *Puma concolor*, one of the largest extant South American carnivores, whose average body mass is 60 kg (Silva & Downing 1995). The equations based on craniodental variables have the lowest values of %SEE, but the resulting body mass is probably

Table 1. Body mass estimation of *Australohyaena antiqua* (UNPSJB PV 113).

Regression	Variable	%SEE	%PE	Adjusted R^2	Smearing estimate	Body mass (kg)
Log y = −1.098 + 3.35 (log x)	UMORL	19	14	0.996	1.2	1241.35
Log y = −1.225 + 3.34 (log x)	LMORL	20	16	0.995	1.6	1603.52
Log y = −2.722 + 3.207 (log x)	TJL	26	18	0.991	2.3	175.28
Ln y = 1.89 + 3.14 (ln x)	M2L	38	7	0.95	1.16	44.13
Ln y = 1.76 + 3.17 (ln x)	m3L	39	12	0.95	1.11	67.08

Table 2. Morphometric indexes used for diet estimation of *Australohyaena antiqua* (UNPSJB PV 113).

Index /variable	RGA	PS	RPS	RPL	TLC	JD	M2L (mm)	m3L (mm)	UOMRL (mm)	LOMRL (mm)	TJL (mm)	Talonid type
Value	0.17	0.65	2.32	0.59	0.91	64.8	16.7	18.7	132.8	145.7	235	I

overestimated (Table 1) because the specimen UNPSJB PV 113 is an outlier in the range values of the independent variables of the equations of Myers (2001).

Diet. Tooth measurements. Five morphometric indexes were calculated for UNPSJB PV 113. The relative grinding area (RGA) (Van Valkenburgh 1991) is the ratio between the square root of the talonid area and the length of the trigonid of the carnassials, and measures the grinding capacity of the molars. The critical values are: RGA < 0.5 = hypercarnivores; RGA $0.5-0.8$ = mesocarnivores, and RGA >0.8 = hypocarnivores (Zimicz 2012). In the case of metatherians, the m4 is used to estimate the RGA following Prevosti *et al*. (2013). The RGA for UNPSJB PV 113 is 0.17 (Table 2), which supports hypercarnivorous habits.

The premolar shape (PS) (Van Valkenburgh 1991) is the ratio between the maximum width and length of the largest lower premolar. It measures the robustness of the premolar and its capacity as a cracking or shearing tool. This index discriminates hypercarnivorous bone-crackers with PS $>$ 0.58 from the remaining carnivorous types with PS $<$ 0.58 (Zimicz 2012). The PS for UNPSJB PV 113 is 0.65 (Table 2) and defines a bone-cracker morphotype.

The relative premolar size (RPS) (Van Valkenburgh 1991) measures the robustness of the premolar considering the body mass. The index is defined as the ratio between the maximum width of the largest lower premolar and the cubic root of the estimated body mass. Similar to PS, this index discriminates hypercarnivorous bone-crackers with RPS $>$ 2.6 from the remaining carnivorous types with RPS $<$ 2.6 (Zimicz 2012). The RPS for UNPSJB PV 113 is 2.32 and groups the specimen with the cat-like species.

The relative premolar length (RPL) (Van Valkenburgh 1991) measures the size of the largest premolar and the carnassial molar. The index is defined as the length of the largest lower premolar over the length of the carnassial molar and discriminates between hypercarnivores with RPL $>$ 0.7 and mesocarnivores and hypocarnivores with RPL $<$ 0.7 (Zimicz 2012). Contrary to the other indexes, the RPL value obtained for UNPSJB PV 113 (0.59; Table 2) suggests mesocarnivorous–hypocarnivorous habits.

The trigonid length of the carnassial molar (TLC) (Van Valkenburgh 1991) estimates the shearing capacity of the carnassials and is the length of the trigonid over the total length of the carnassial molar. The critical values discriminate: hypercarnivorous cat-like with TLC $>$ 0.9; hypercarnivorous bone-crackers with $0.8 <$ TLC < 0.9; mesocarnivores with $0.7 <$ TLC < 0.8; and hypocarnivores with TLC < 0.7 (Zimicz 2012). The TLC for UNPSJB PV 113 of 0.91 (Table 2) suggests hypercarnivorous cat-like habits, although very close to the boundary with bone-cracker forms.

Skull measurements. We used the method developed by Werdelin (1989) to infer the diet on the basis of the skull morphology. An arc was traced in the lateral view of the skull and jaw of UNPSJB PV 113, with the upper and lower molars in occlusion (Fig. 8A). The centre of the circle was placed in the point of rotation of the lower jaw (condyle). The radius is equal to the distance between the condyle and the apex of the cracking tooth (p3). The arc passes between the infraorbital foramen and the anteroventral surface of the orbit continuing up to the skull roof (Werdelin 1989). The arc in UNPSJB PV 113 was almost tangential to the skull roof (Fig. 8A), with an angle of 14°. This is similar to bone-crackers with vaulted skulls, such as hyaenas (*Crocuta crocuta*) and the fossil bone-cracker canid *Osteoborus cyonoides* (Werdelin 1989). The arc in *C. crocuta* and *Hyaena brunnea* contacts

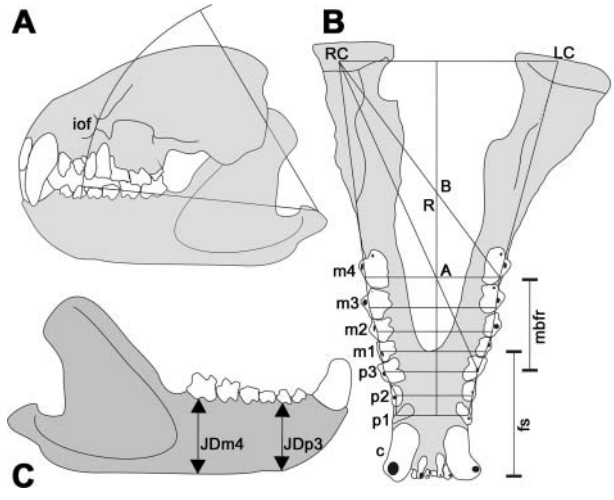

Figure 8. Skull and jaw measurements of *Australohyaena antiqua*. **A,** lateral view of the anterior portion of the skull showing its vaulted appearance; **B,** jaw geometry after Werdelin (1989); **C,** lateral view of the right dentary. Abbreviations: iof, infraorbital foramen; fs, fused symphysis; LC, left condyle; mbfr, maximum bite force region; A, position of the resultant force at the cracking tooth; B, position of the resultant force at the carnassials; R, position of the resultant bite force; RC, right condyle; JD, jaw depth.

the skull roof at 10° and 15°, respectively (N. Zimicz, pers. obs.). The vaulted skull has the function to withstand the compressive forces generated during the bite at the level of premolars (Buckland-Wright 1978). In the cat-like and wolf-like hypercarnivores and mesocarnivores, the arc passes above the skull roof in an obtuse angle (Werdelin 1989). *Panthera* species have contact angles varying from 17° (*P. leo*) to 28° (*P. pardus*). *Panthera tigris* and *P. onca* have angles between 25° and 26° respectively (N. Zimicz, pers. obs.).

Jaw measurements. We used the geometry of the lower jaw of UNPSJB PV 113 (Fig. 8B) to test the diet estimations (Greaves 1983, 1985; Werdelin 1987, 1989). Bone-crackers concentrate the bite force at the level of the cracking premolars while other carnivores produce the optimal level of force at the carnassials. The method consists of a series of lines connecting functional points of the mandibles in occlusal view (Fig. 8B). RC and LC are the midpoints of the right and left condyles respectively; A represents the anteriormost position of the jaw muscle resultant, and B is the point at which a line connecting the last molar with the opposite condyle crosses the midline of the jaw (Fig. 8B). The area between the lines RC-A and RC-B is the zone of maximum muscle force and R is the expected muscle resultant position at the carnassials. In UNPSJB PV 113 the maximum force zone is between the posterior root of p2 and m4 (Fig. 8B), and p3 lies entirely on the zone of the jaw where the bite force is maximal, as occurs in extant hyaenas (Werdelin 1989). The use of p3 as a cracking tooth is also supported in the UNPSJB PV 113 by the extension of the mandibular symphysis to the anterior root of m1. The p3 is included totally over the fused region of the symphysis, suggesting that heavy loads can be supported by this area (Fig. 8B).

Bone-crackers have deeper dentaries and smaller differences in the jaw depth at the cracking premolar and carnassial molar than other carnivores (Palmqvist *et al.* 2011), as is the case in UNPSJB PV 113 (Fig. 8C). The dentary is 3.5 mm higher at the level of m4 than at the level of p3. The difference is slightly more stressed at the lingual side with 7.5 mm difference (measurements in Supplemental Material). Considering the jaw depth as a function of the body mass (Fig. 9) and the estimation at 67 kg (Table 1) for UNPSJB PV 113, the dentary of this specimen is more robust than the giant fossil hyaena *Pachycrocuta brevirostris* (Palmqvist *et al*. 2011, p. 11) and similar to *Proborhyaena gigantea*, a probable bone-cracker sparassodont of Deseadan age (Fig. 9).

Palaeoecology of *Australohyaena antiqua* and comparisons with other Deseadan sparassodonts. The analysis of UNPSJB PV 113 places *A. antiqua* among hypercarnivores, as suggested by comparing the values obtained with the RGA, PS, RPS and TLC morphometric indexes. The only estimation that suggests

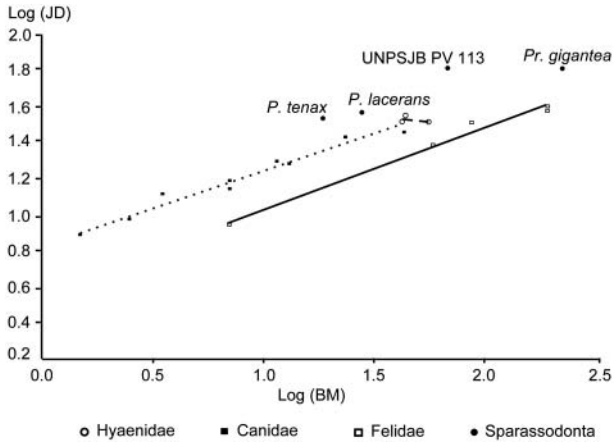

Figure 9. Scatter plot of the log transformed jaw depth (JD) and body mass (BM) in a sample of living placental carnivores and Deseadan Sparassodonta.

mesocarnivorous–hypocarnivorous habits is the RPL. The value of 0.59 obtained for UNPSJB PV 113 is distant from the average for hypercarnivores. Although, 20 living hypercarnivore species have point values of this index between 0.54 and 0.97 (Zimicz 2012). In this sense, we consider that the RPL index is less reliable than others as a diet predictor. Excluding *Pharsophorus tenax*, which lies on the limit of mesocarnivory, other Deseadan sparassodonts have RGA and RPS values that suggest hypercarnivorous habits (Zimicz 2012). In addition, *P. tenax* have the lowest TLC values for the genus that lies in the limit of mesocarnivory (Zimicz 2012). *Fredszalaya hunteri* from the Deseadan beds of Salla (Bolivia; Shockey & Anaya 2008) has no preserved lower dentition and no morphometric index can be calculated. The interpretation as a hypercarnivore is based on *Prothylacynus* (Prevosti *et al.* 2013), which shares a similar upper dentition (Shockey & Anaya 2008).

The PS value (Table 2) and the results of the analysis of the skull and jaws suggest that UNPSJB PV 113 was a bone-cracker. Conversely, the RPS (calculated with a body mass of 67 and 44 kg) and the TLC values (Table 2) suggest a cat-like type. Considering the obtained values together with the vaulted appearance of the skull, the jaw geometry, the robustness of the dentary, the strong development of the temporal musculature (suggested by the high sagittal crest, deep depressions on the squamosal dorsal to the glenoid cavity for the muscular attachment, and large foramina on the squamosal for blood drainage), and the robustness of p3, we believe that the most likely hypothesis is that UNPSJB PV 113 occupied the hyaena-like ecomorph *sensu* Van Valkenburgh (2007). The Deseadan *P. lacerans* and *P. tenax* have values that are in the range of cat-like forms for PS (0.52 and 0.48 respectively). The hathliacynids *Notogale mitis* and *Sallacyon hoffstetteri* have a cuspate talonid on their lower molars

Table 3. Palaeoecological reconstruction of Deseadan sparassodonts. Palaeobiological inferences were taken from Zimicz (2012) and Prevosti *et al*. (2013). Palaeoecology of *Australohyaena antiqua* is discussed in the text. Body mass calculation of *Fredszalaya hunteri* is in the Supplemental Material.

Taxon	Diet	Body mass
Notogale mitis	Hypercarnivores – wolf-like	Small size (~1 to 3 kg)
Sallacyon hoffstetteri	Hypercarnivores – wolf-like	Small size (~1 to 3 kg)
Fredszalaya hunteri	Hypercarnivores	Medium size (~10 kg)
Pharsophorus tenax	Limit to mesocarnivory	Large size (~15 to 20 kg)
Pharsophorus lacerans	Hypercarnivores – cat-like	Large size (~ 30 kg)
Australohyaena antiqua	Hypercarnivores – bone-cracker	Large size (67 kg)
Proborhyaena gigantea	Hypercarnivores – bone-cracker	Large size (~ 90 to 100 kg)
Paraborhyaena boliviana	Hypercarnivores – bone-cracker	Large size (~ 90 kg)

similar to the trenchant heel of wolf-like hypercarnivores (Zimicz 2012). *Proborhyaena gigantea* has several features of bone-crackers (deep jaw depth, fused symphysis extending to the p3–m1 joint, and robust cracking premolar with PS = 0.6; Zimicz 2012). The palaeoecological restoration of *Paraborhyaena boliviana* is incomplete because the dentition is eroded for estimating the morphometric indexes. However some morphological traits, such as the fused symphysis extending to the anterior root of m1, and the massive aspect of their lower third premolar, suggest that it was another bone-cracker (Table 3).

The estimated body mass of UNPSJB PV 113 of 67 kg lies in the range of values of *Arctodictis munizi* from the younger Santacrucian beds (Ercoli & Prevosti 2011; Ercoli *et al.* 2013). Dental variables are considered poor estimators of body mass compared to postcranial variables (Damuth & MacFadden 1990), and the sparassodonts are no exception (Prevosti *et al.* 2013). However, the scarcity of postcranial elements requires dependence on the dental indexes for the group. Deseadan sparassodonts range from small to large sizes (Table 3). *Sallacyon hoffstetteri* and *Notogale mitis* were the smallest Deseadan sparassodonts at about 1 to 3 kg (Zimicz 2012; Prevosti *et al*. 2013). The largest was *Proborhyaena gigantea* at about 100 kg (93 or 153 kg according to Zimicz 2012 and Prevosti *et al.* 2013, respectively).

Homology of the lower tooth cusps in Borhyaenidae

The occurrence of the metaconid in the lower molars in Sparassodonta has been discussed for the species of Borhyaenidae. Marshall (1978) considered that the metaconid is present in basal forms, but it is lost in post-Deseadan borhyaenids. This idea was questioned by Goin *et al.* (2007), who considered that either the cusp posterior to the protoconid is homologous to the entoconid or the entoconid is fused to the metaconid. We support here the interpretation of the posterior cusp being homologous to the metaconid for the m2–m4 or m2–m3 of *Pharsophorus*, *Borhyaena*, *Australohyaena* and *Arctodictis* (see Phylogeny section).

Basal sparassodonts such as *Patene* or *Nemolestes* show a primitive molar pattern with complete trigonid and talonid cusps (Fig. 10A). The trigonid is tricuspate, with a reduced metaconid located at the distolingual corner of the trigonid. The talonid is wide (as wide as the trigonid), with the hypoconid, entoconid, hypoconulid and associated crests. The postcingulid descends from the hypoconulid and surrounds labially the base of the hypoconid.

Pharsophorus lacerans has a more specialized carnivorous dentition. The m1 of *Pharsophorus* (Figs 10B, 11D) lacks a metaconid and the trigonid is formed by the paraconid and protoconid aligned with the mesiodistal axis of the tooth. The talonid is short, narrower than the base of the protoconid, basined, and cuspate. The tallest cusp of the talonid is the hypoconid placed nearly on the sagittal axis of the tooth. The entoconid is small. The hypoconulid is minute, located in a median position in the distal border of the talonid. The postcingulid descends from the hypoconulid to the distolabial border of the crown. This tooth morphology is similar to that of the lower molars of hathliacynids, *Pseudothylacynus* and *Prothylacynus* (Fig. 11A–C) in that all molars lack a metaconid, possess a basined three-cuspate talonid, and a well-developed postcingulid. Unlike the m1, the trigonid of the m2 in *Pharsophorus* (Figs 10B, C, 11D) has a small metaconid located on the distolingual side of the protoconid, resembling basal sparassodonts. The metaconid is a conical cusp, almost circular in cross section. The postprotocristid descends from the tip of the protoconid to the metaconid; there is a carnassial notch between both cusps. The talonid is slightly wider than long and basined. The surface of the talonid is lingually inclined (the base of the hypoconid is lower than the base of the entoconid). The hypoconid is considerably lower than in the m1. There is a crest that surrounds the distal border of the talonid connecting the entoconid and the hypoconid. This crest should include the hypoconulid, but the cusp is not evident in this tooth. The entoconid is small, labiolingually compressed,

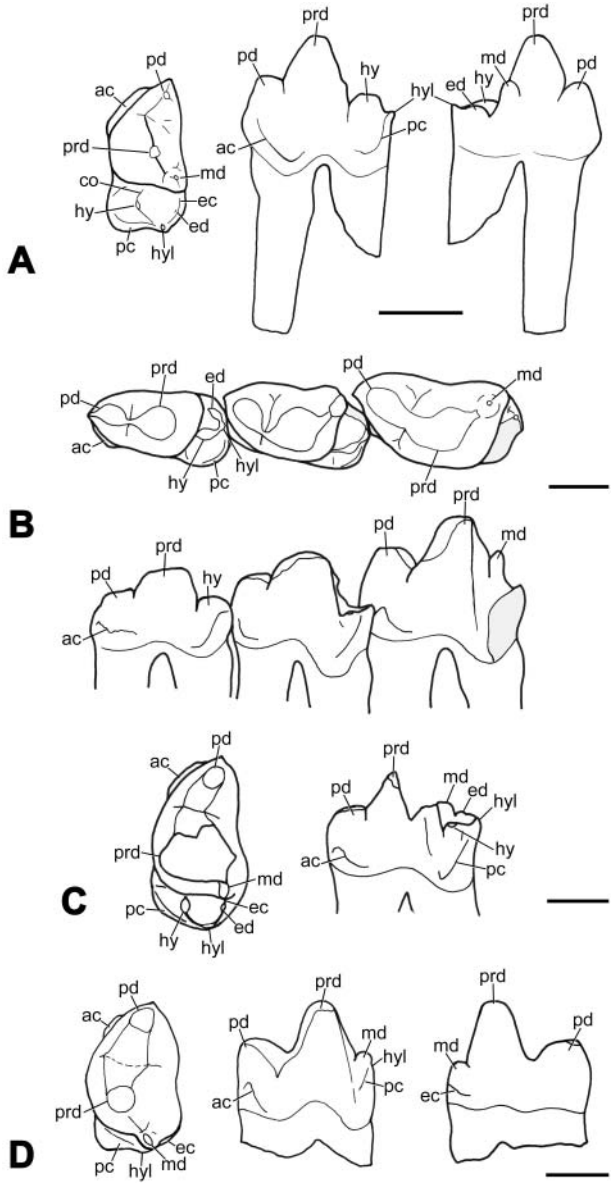

Figure 10. Line drawing of lower molars. **A,** left lower molar of cf. *Nemolestes* sp. (AMNH 29433), in occlusal, labial and lingual views; **B,** left m1−m3 of *Pharsophorus lacerans* (MACN A 11652), in occlusal and labial views; **C,** left m2 of *Pharsophorus lacerans* (MACN A 52-391), in occlusal and labial views; **D,** left m3 of *Borhyaena tuberata* (MACN A 9342), in occlusal and labial views. Abbreviations: ac, anterior cingulum; co, cristid obliqua; ec, entocristid; ed, entoconid; hy, hypoconid; hyl, hypoconulid; md, metaconid; pc, postcingulid; pd, paraconid; prd, protoconid. Scale bar in A: 2 mm; B−E: 5 mm.

continuous with the entocristid and located on the lingual border of the talonid. There is a notch between the entocristid and the metaconid. The m3 has a similar pattern (Figs 10B, 11D). The metaconid has a higher position in the m3 than that in the m2. The labial inclination of the talonid surface is emphasized in the m3. Only the hypoconid and the very compressed entoconid are recognized in the talonid. The m4 has a strongly reduced talonid (Fig. 11D). The entoconid is vestigial and located distolabial to the metaconid. The postcingulid descends towards the base of the crown. *Plesiofelis* (Fig. 11E) has a cusp arrangement similar to *Pharsophorus* (Cabrera 1927; Simpson 1948; Marshall 1978; alternative view in Goin *et al.* 2007). The main differences consist of the proportion of the cusps and arrangement of crests.

Based on the morphology described and on the phylogenetic context, the lower molars of the borhyaenids *Australohyaena*, *Borhyaena* and *Arctodictis* (Figs 6B, 10D, 11F) are interpreted as follows. The m1 has a paraconid and protoconid that are aligned with the anteroposterior axis of the tooth as in *Pharsophorus*. Posterior to the protoconid there is a cusp, slightly smaller than the paraconid, aligned to the paraconid−protoconid axis and to the sagittal axis of the tooth, which is interpreted as an enlarged hypoconid, based on the morphology of the m1 of *Pharsophorus*. The entoconid is absent in most of the specimens analysed (only *Borhyaena* MACN A 9341-42 has a vestigial cusp). The distolingual border of the tooth is closed by a crest that directs to the lingual base of the protoconid and would be homologous to the entocristid. The postcingulid is broad and descends from the distolabial margin of the tooth to the ventral border of the distal lobe of the crown.

The m2 and m3 of borhyaenids (Figs 6B, 10D, 11F) have a paraconid, protoconid and a distolingual cusp. This cusp is interpreted as homologous to the metaconid, observed in the m2−m4 of *Pharsophorus* and basal sparassodonts. A postprotocristid descends from the apex of the protoconid to the base of the metaconid and has a deep carnassial notch. There is a wear facet developed on the distolabial face of the protoconid and the metaconid identified as facet 1 of Crompton (1971). The short and oblique orientation of this facet is in agreement with that observed on the preparacrista of the upper molars. The talonid is vestigial and there is a disconnection with the trigonid structures. A crest borders the tooth distolingually, bordering the base of the protoconid that could be homologous to the entocristid. The postcingulid descends labially from the middle of the tooth. In some specimens, there is a vestigial cusp on the sagittal axis of the posterior border of the talonid, from which the postcingulid descends. This cusp should be homologous with the hypoconulid, observed in *Pharsophorus*. The vestigial talonid of borhyaenids is in concordance with the vestigial upper molar protocones. The m4 paraconid and protoconid are taller. The metaconid is vestigial and observed at the distolingual base of the protoconid (*Australohyaena*; Fig. 6B), or it is absent (*Borhyaena*, *Arctodictis*; Fig. 11F), with vestigial or no evidence of talonid.

In summary, the morphological tendency of the lower molars evident in the borhyaenoid lineage is for disconnection of the talonid and trigonid, and reduction of the

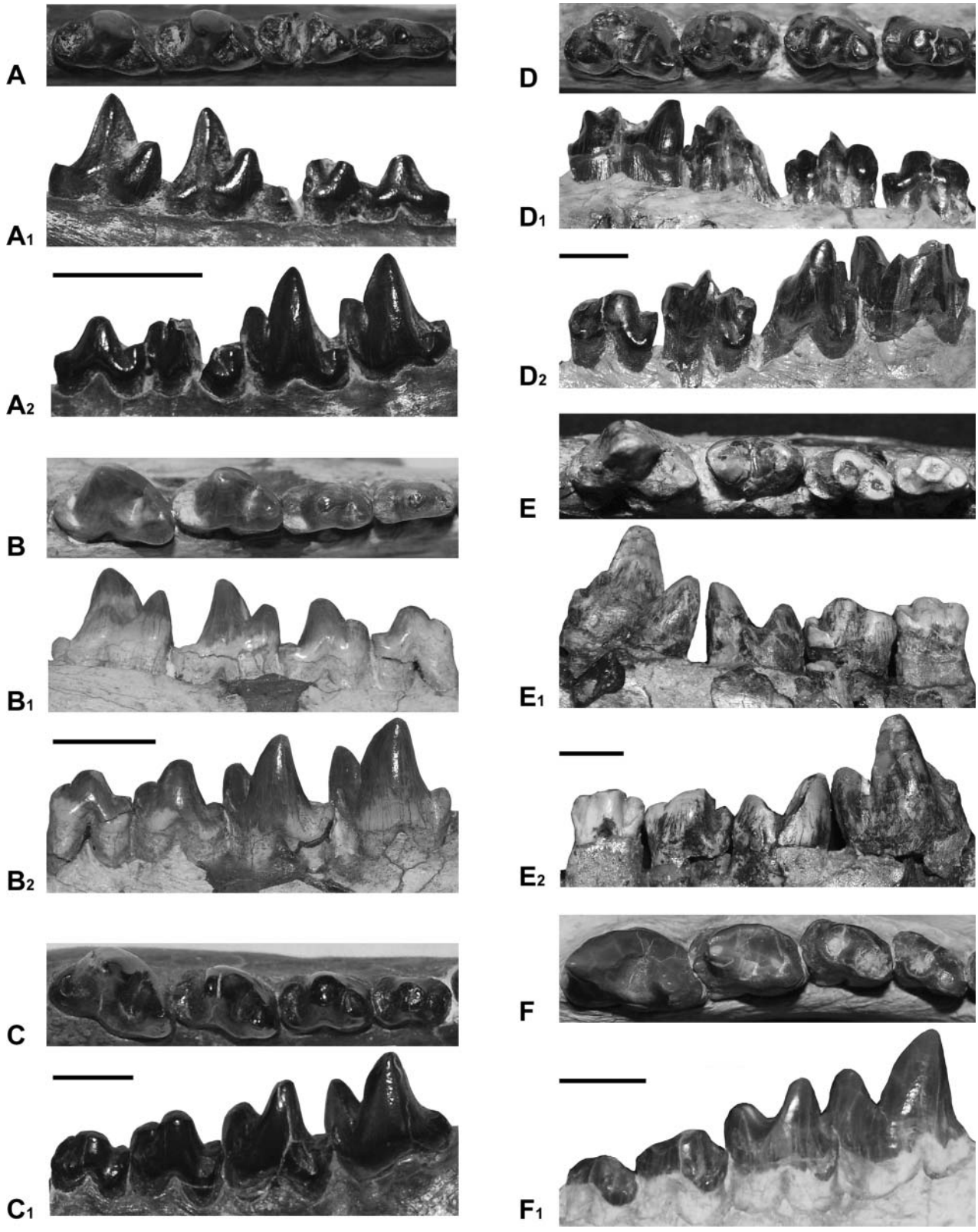

Figure 11. Lower molars of sparassodonts without metacone (**A**–**C**) and with metacone on m2–m4 or m2–m3 (**D**–**F**). **A,** *Sipalocyon gracilis* (MACN A 691–703, inverted right mandibule) in occlusal, lingual and lateral views; **B,** *Pseudothylacynus rectus* (MACN A 52-369) in occlusal, lingual and labial views; **C,** *Prothylacynus patagonicus* (MACN A 706–720) in occlusal and labial views; **D,** *Pharsophorus lacerans* (MACN A 52-391) in occlusal, lingual and labial views; **E,** *Plesiofelis schlosseri* (MLP 11-114) in occlusal, lingual and labial views; **F,** *Arctodictis sinclairi* (MLP 85-VII-3-1) in occlusal and labial views. Scale bar: 10 mm.

talonid in favour of the development of the trigonid. Functionally, the shearing areas of the tooth increase in size, such as the paracristid and metacristid in the lower and the postmetacrista and preparacrista in the upper molars. Grinding areas are vestigial to absent, such as the talonid in the lower and protocone in the upper molars.

If the interpretations about the homologies supported in this contribution are correct, there is a clear difference in tooth patterns between m1 and m2–m4 in the Borhyaenidae. In the phylogenetic context, the presence of the metaconid is a plesiomorphic trait, while its absence is the derived state. The metaconid is present in all the molars in plesion metatherians and most marsupials. The Sparassodonta hathliacynid and some basal borhyaenoids (e.g. *Lycopsis* and *Prothylacynus*) lack the metaconid in the entire molar series. Borhyaenidae has the metaconid on all molars except m1, which suggests that among the lower molars m1 is an evolutionary plastic tooth for acquiring major morphological change. A similar discrepancy in the morphology of the first molar compared to the posterior elements has been reported in marsupials. For example, *Sarcophilus* lacks the paraconid on the m1 but this cusp is present in the posterior molars and shifts posteriorly the premolariform–molariform boundary (Archer 1976). If the seven postcanine teeth of eutherians and metatherians are homologous and the first molar of metatherians is homologous to the deciduous premolar (dP4/dp4; Luckett 1993; O'Leary *et al*. 2013) of Eutheria, then this would result in metatherians presenting different morphological constraints between first and posterior molars.

Tooth morphology, the presence, absence, arrangement and sizes of cusps are variables in mammals. In developing teeth, the enamel knots act as epithelial signalling centres to control cusp positions and are the first signs of cusp patterns that distinguish species (Kassai *et al.* 2005; Jernvall & Thesleff 2012). The gene system regulating the tooth development is highly complex, but the network organization requires a few small changes and simple activator–inhibitor feedback loops to generate different crown types and cusp patterns (Kassai *et al.* 2005; Salazar-Ciudad & Jernvall 2002, 2010). Homoplasies are frequent in mammals and this makes interpretation of homologies and the character evolution a controversial issue.

Conclusions

A new taxonomic combination is proposed for *Australohyaena antiqua* (Ameghino) on the basis of its phylogenetic affinities, which places it as member of the Borhyaenidae (Mammalia, Metatheria, Sparassodonta), distant from *Pharsophorus lacerans*, the genus to which it was formerly referred. A unique combination of features clearly differentiates *A. antiqua* from other sparassodonts. An emended diagnosis is provided considering characters from the skull, dentary and dentition.

The craniodental characteristics of *Australohyaena antiqua* suggest that it was a hypercarnivore predator. Several features (vaulted skull, well-developed temporal fossa and consequently temporal musculature, and high jaw at the carnassial and p3) are suggestive of bone-cracker capabilities.

The body mass estimation provides a value of about 70 kg and places *A. antiqua* within the largest Deseadan sparassodonts.

We support the interpretation that the cusp posterior to the protoconid is homologous to the hypoconid in the m1 but the cusp posterior to the protoconid in m2–m4 is homologous to the metaconid in the posterior molars in Borhyaenidae.

Acknowledgements

We gratefully thank Mónica Abril (UNPSJB) for permitting access to the specimen of *Australohyaena antiqua* and her courteous support during the study of the material. We thank M. Reguero (MLP) and A. Kramarz (MACN), for permitting access to the collections under their care; Enrique Guanuco (Fundación Miguel Lillo) for the drawings, G. W. Rougier for his guidance on the study of mammal anatomy and S. D. Kay who kindly assisted by reviewing the English in early versions of the manuscript. The anonymous reviewers and editors provided useful suggestions. This is a contribution to the project financially supported by PICT 2010-1805, PICT 2011-0309, PIP 1723 CONICET, and IPA-P.1, Fundación Miguel Lillo. We acknowledge having used the Willi Hennig Society edition of TNT.

Supplemental data

Supplemental material for this article can be accessed here: http://dx.doi.org/10.1080/14772019.2014.926403

References

Ameghino, F. 1894. Enumération synoptique des espèces de mammifères fossiles des formations éocènes de Patagonie. *Boletín de la Academia Nacional de Ciencias de Córdoba*, **13**, 259–452.

Ameghino, F. 1897. Mammifères Crétacés de l'Argentine. Deuxième contribution à la connaissance de la faune mammalogique des conches à *Pyrotherium*. *Boletín del Instituto Geográfico Argentino*, **18**, 406–521.

Archer, M. 1976. The dasyurid dentition and its relationships to that of didelphids, thylacinids, borhyaenids (Marsupicarnivora) and peramelids (Peramelina: Marsupialia). *Australian Journal of Zoology, Supplementary Series*, **39**, 1–34.

Babot, M. J. 2005. *Los Borhyaenoidea (Mammalia, Metatheria) del Terciario inferior del Noroeste argentino. Aspectos filogenéticos, paleobiológicos y bioestratigráficos*. Unpublished PhD thesis, Universidad Nacional de Tucumán, 454 pp.

Babot, M. J., **Powell, J. E.** & **Muizon, C de.** 2002. *Callistoe vincei*, a new Proborhyaenidae (Borhyaenoidea, Metatheria, Mammalia) from the early Eocene of Argentina. *Geobios*, **35**, 615–629.

Bond, M. & **Pascual, R.** 1983. Nuevos y elocuentes restos craneanos de *Proborhyaena gigantea* Ameghino, 1897 (Marsupialia, Borhyaenidae, Proborhyaeninae) de la Edad Deseadense. Un ejemplo de coevolución. *Ameghiniana*, **20**, 47–60.

Buckland-Wright, J. C. 1978. Bone structure and the patterns of force transmission in the cat skull (*Felis catus*). *Journal of Morphology*, **155**, 35–62.

Cabrera, A. 1927. Datos para el conocimiento de los dasyuroideos fósiles argentinos. *Revista del Museo de La Plata*, **30**, 271–315.

Cerdeño, E. 2011. Quebrada Fiera (Mendoza), an important paleobiogeographic center in the South American late Oligocene. *Estudios Geológicos*, **67**, 375–384.

Chaffee, R. G. 1952. The Deseadan vertebrate fauna of the Scarritt Pocket, Patagonia. *Bulletin of the American Museum of Natural History*, **98**, 507–562.

Crompton, A. W. 1971. The origin of the tribosphenic molar. *Zoological Journal of the Linnean Society*, **50**, Supplement 1, 65–87.

Damuth, J. & **Macfadden, B.** 1990. Body size and its estimation. Pp. 1–10 in J. Damuth & B. J. Macfadden (eds) *Body size in mammalian paleobiology. Estimation and biological implications*. Cambridge University Press, Cambridge.

Dunn, R. E., **Madden, R. H.**, **Kohn, M. J.**, **Schmitz, M. D.**, **Strömberg, C. A. E.**, **Carlini, A. A.**, **Ré, G. H.** & **Crowley, J.** 2012. A new chronology for middle Eocene–early Miocene South American Land Mammal Ages. *Bulletin of the Geological Society of America*, **125**, 539–555.

Engelman, R. K. & **Croft, D. A.** 2014. A new species of small-bodied sparassodont (Mammalia: Metatheria) from the middle Miocene locality of Quebrada Honda, Bolivia. *Journal of Vertebrate Paleontology*, **34**, 672–688.

Ercoli, M. D. & **Prevosti, F. J.** 2011. Estimación de masa de las especies de Sparassodonta (Mammalia, Metatheria) de la edad santacrucense (Mioceno temprano) a partir del tamaño del centroide de los elementos apendiculares: inferencias paleoecológicas. *Ameghiniana*, **48**, 462–479.

Ercoli, M. D., **Prevosti, F. J.** & **Forasiepi, A. M.** 2013. The structure of the mammalian predator guild in the Santa Cruz Formation (late early Miocene), Patagonia, Argentina. *Journal of Mammalian Evolution*, DOI:10.1007/s10914-013-9243-4.

Evans, H. E. & **Christensen, G. C.** 1979. *Anatomy of the dog*. Saunders Publisher, Philadelphia, 941 pp.

Forasiepi, A. M. 2009. Osteology of *Arctodictis sinclairi* (Mammalia, Metatheria, Sparassodonta) and phylogeny of Cenozoic metatherian carnivores from South America. *Monografías del Museo Argentino de Ciencias Naturales n.s.*, **6**, 1–174.

Forasiepi, A. M., **Sánchez-Villagra, M. R.**, **Goin, F. J.**, **Takai, M.**, **Shigehara, N.** & **Kay, R. F.** 2006. A new species of Hathliacynidae (Metatheria, Sparassodonta) from the Middle Miocene of Quebrada Honda, Bolivia. *Journal of Vertebrate Paleontology*, **26**, 670–684.

Goin, F. J., **Sánchez-Villagra, M. R.**, **Abello, A.** & **Kay, R. F.** 2007. A new generalized paucituberculatan marsupial from the Oligocene of Bolivia and the origin of 'shrew-like' opossums. *Palaeontology*, **50**, 1267–1276.

Goin, F. J., **Abello, M. A.** & **Chornogubsky, L.** 2010. Middle Tertiary marsupials from central Patagonia (early Oligocene of Gran Barranca): understanding South America's Grande Coupure. Pp. 69–105 in R. H. Madden, A. A. Carlini, M. G. Vucetich & R. F. Kay (eds) *The paleontology of Gran Barranca: evolution and environmental change through the Middle Cenozoic of Patagonia*. Cambridge University Press, Cambridge.

Goloboff, P. A. 1993. Estimating character weight during tree search. *Cladistics*, **9**, 83–91.

Goloboff, P., **Carpenter, J. M.**, **Arias, S. J.** & **Miranda Esquivel, D. R.** 2008a. Weighting against homoplasy improves phylogenetic analysis of morphological data sets. *Cladistics*, **24**, 1–16.

Goloboff, P. A., **Farris, J. S.** & **Nixon, K. C.** 2008b. T.N.T., a free program for phylogenetic analysis. *Cladistics*, **24**, 774–786.

Gordon, C. L. 2003. A first look at estimating body size in dentally conservative marsupials. *Journal of Mammalian Evolution*, **10**, 1–21.

Greaves, W. S. 1983. A functional analysis of carnassial biting. *Biological Journal of the Linnean Society*, **20**, 353–363.

Greaves, W. S. 1985. The generalized carnivore jaw. *Zoological Journal of the Linnean Society*, **85**, 267–274.

Hershkovitz, P. 1982. The staggered marsupial lower third incisor (i3). *Geobios, Mémoire Spécial*, **6**, 191–200.

Hershkovitz, P. 1995. The staggered marsupial third lower incisor: hallmark of Cohort Didelphimorphia, and description of a new genus and species with staggered i3 from the Albian (Lower Cretaceous) of Texas. *Bonner Zoologische Beiträge*, **45**, 153–169.

Hiatt, J. L. & **Gartner, L. P.** 1987. *Textbook of head and neck anatomy*. 3rd edition. Lippincott Williams and Wilkins, Philadelphia, 352 pp.

Huxley, J. S. 1880. On the application of the law of evolution to the arrangement of the Vertebrata and more particular to the Mammalia. *Proceedings of the Zoological Society of London*, **43**, 649–662.

Jernvall, J. & **Thesleff, I.** 2012. Tooth shape formation and tooth renewal: evolving with the same signals. *Development*, **139**, 3487–3497.

Kassai, Y., **Munne, P.**, **Hotta, Y.**, **Penttilä, E.**, **Kavanagh, K.**, **Ohbayashi, N.**, **Takada, S.**, **Thesleff, I.**, **Jernvall, J.** & **Itoh, N.** 2005. Regulation of mammalian tooth cusp patterning by ectodin. *Science*, **309**, 2067–2070.

Koyabu, D., **Maier, W.** & **Sánchez-Villagra, M. R.** 2012. Paleontological and developmental evidence resolve the homology and dual embryonic origin of a mammalian skull bone, the interparietal. *Proceedings of the National Academy of Sciences*, **109**, 14075–14080.

Krajewski, C., **Driskell, A. C.**, **Baverstock, P. R.** & **Braun, M. J.** 1992. Phylogenetic relationships of the thylacine (Mammalia: Thylacinidae) among dasyuroid marsupials: evidence from cytochrome b DNA sequences. *Proceedings of the Royal Society of London, Series B*, **250**, 19–27.

Krajewski, C., **Buckley, L.** & **Westerman, M.** 1997. DNA phylogeny of the marsupial wolf resolved. *Proceedings of the Royal Society of London, Series B*, **264**, 911–917.

Ladevèze, S. & **Muizon, C. de.** 2010. Evidence of early evolution of Australidelphia (Metatheria, Mammalia) in South America: phylogenetic relationships of the metatherians from the late Palaeocene of Itaboraí (Brazil) based on teeth and petrosal bones. *Zoological Journal of the Linnean Society*, **159**, 746–784.

Loomis, F. B. 1914. *The Deseado Formation of Patagonia*. Amherst College, New Haven, 232 pp.

Luckett, W. P. 1993. Ontogenetic staging of the mammalian dentition, and its value for assessment of homology and heterochrony. *Journal of Mammalian Evolution*, **1**, 269–282.

Macrini, T. E., **Muizon C. de**, **Cifelli, R. L.** & **Rowe, T.** 2007. Digital cranial endocast of *Pucadelphys andinus*, a Paleocene metatherian. *Journal of Vertebrate Paleontology*, **27**, 99–107.

Marshall, L. G. 1978. Evolution of the Borhyaenidae, extinct South American predaceous marsupials. *University of California Publications in Geological Sciences*, **117**, 1–89.

Mones, A. & **Ubilla, M.** 1978. La edad Deseadense (Oligoceno inf.) de la Formación Fray Bentos y su contenido paleontológico con especial referencia a la presencia de *Proborhyaena* cf. *gigantea* Ameghino (Marsupialia: Borhyaenidae) en el Uruguay. Nota preliminar. *Comunicaciones Paleontológicas del Museo de Historia Natural de Montevideo*, **1**, 151–158.

Muizon, C. de. 1998. *Mayulestes ferox*, a borhyaenoid (Metatheria, Mammalia) from the early Paleocene of Bolivia. Phylogenetic and palaeobiologic implications. *Geodiversitas*, **20**, 19–142.

Muizon, C. de. 1999. Marsupial skulls from the Deseadan (late Oligocene) of Bolivia and phylogenetic analysis of the Borhyaenoidea (Marsupialia, Mammalia). *Geobios*, **32**, 483–509.

Myers, T. J. 2001. Prediction of marsupial body mass. *Australian Journal of Zoology*, **49**, 99–118.

O'Leary, M. A., **Bloch, J. I.**, **Flynn, J. J.**, **Gaudin, T. J.**, **Giallombardo, A**, **Giannini, N. P.**, **Goldberg, S. L.**, **Kraatz, B. P.**, **Luo, Z.-X.**, **Meng, J.**, **Ni, X.**, **Novacek, M. J.**, **Perini, F. A.**, **Randall, Z. S.**, **Rougier, G. W.**, **Sargis, E. J.**, **Silcox, M. T.**, **Simmons, N. B.**, **Spaulding, M.**, **Velazco, P. M.**, **Weksler, M.**, **Wible, J. R.** & **Cirranello, A. L.** 2013. The placental mammal ancestor and the post–K-Pg radiation of placentals. *Science*, **339**, 662–667.

O'Meara, R. N. & **Thompson, R. S.** 2014. Were there Miocene Meridiolestidans? Assessing the phylogenetic placement of *Necrolestes patagonensis* and the presence of a 40 million year Meridiolestidan ghost lineage. *Journal of Mammalian Evolution*, DOI: 10.1007/s10914-013-9252-3.

Palmqvist, P., **Martínez-Navarro, B.**, **Pérez-Claros, J. A.**, **Torregrosa, V.**, **Figuerido, B.**, **Jiménez-Arenas, J. M.**, **Patrocinio Espigares, M.**, **Ros-Montoya, S. Y** & **De Renzi, M.** 2011. The giant hyena *Pachycrocuta brevirostris*: modeling the bone-cracking behavior of an extinct carnivore. *Quaternary International*, **12**, 1–19.

Patterson, B. & **Marshall, L. G.** 1978. The Deseadan, early Oligocene, Marsupialia of South America. *Fieldiana Geology*, **41**, 37–100.

Petter, G. & **Hoffstetter, R.** 1983. Les marsupiaux du Déséadien (Oligocène Inférieur) de Salla (Bolivie). *Annales de Paléontologie (Vert.-Invert.)*, **69**, 175–234.

Pinna, M. G. G. de. 1991. Concepts and tests of homology in the cladistics paradigm. *Cladistics*, **7**, 367–394.

Prevosti, F. J., **Forasiepi, A. M.** & **Zimicz, A. N.** 2013. The evolution of the Cenozoic terrestrial mammalian predator guild in South America: competition or replacement? *Journal of Mammalian Evolution*, **20**, 3–21.

Quiroga, J. C. 1978. El encéfalo de *Borhyaena fera* (Mammalia, Marsupialia). Estudio preliminar sobre las áreas corticales de dos marsupiales extinguidos. *Publicaciones del Museo Municipal de Ciencias Naturales de Mar del Plata "Lorenzo Scaglia"*, **2**, 191–197.

Reguero, M. A. & **Escribano, V.** 1996. *Trachytherus spegazzinianus* Ameghino, 1889 (Notoungulata: Mesotheriidae) de la edad Deseadense Deseadense (Oligoceno superior–Mioceno inferior) de Argentina y Bolivia. *Naturalia Patagónica*, *Revista de la Universidad Nacional de la Patagonia "San Juan Bosco"*, **4**, 43–71.

Salazar-Ciudad, I. & **Jernvall, J.** 2002. A gene network model accounting for development and evolution of mammalian teeth. *Proceedings of the National Academy of Sciences USA*, **99**, 8116–8120.

Salazar-Ciudad, I. & **Jernvall, J.** 2010. A computational model of teeth and the developmental origins of morphological variation. *Nature*, **464**, 583–586.

Sánchez-Villagra, M. R. & **Smith, K. K.** 1997. Diversity and evolution of the marsupial mandibular angular process. *Journal of Mammalian Evolution*, **4**, 119–144.

Schaller, O. 1992. *Illustrated veterinary anatomical nomenclature*. Ferdinand Enke Verlag, Stuttgart, 575 pp.

Shockey, B. C. & **Anaya, F.** 2008. Postcranial osteology of mammals from Salla, Bolivia (late Oligocene): form, function, and phylogenetic implications. Pp. 135–157 in E. J. Sargis & M. Dagosto (eds) *Mammalian Evolutionary Morphology. A Tribute to Frederick S. Szalay*. Springer, Netherlands.

Silva, M. & **Downing, J. A.** 1995. *CRC handbook of mammalian body masses*. CRC Press, Florida, USA, 359 pp.

Simpson, G. G. 1948. The beginning of the age of mammals in South America. Part I. *Bulletin of the American Museum of Natural History*, **91**, 1–232.

Sinclair, W. J. 1906. Mammalia of the Santa Cruz beds: Marsupialia. *Reports of the Princeton University, Expedition to Patagonia*, **4**, 333–460.

Smith, J. B. & **Dodson, P.** 2003. A proposal for a standard terminology of anatomical notation and orientation in fossil vertebrate dentitions. *Journal of Vertebrate Paleontology*, **23**, 1–12.

Soria, M. F. & **Alvarenga, H. M. F.** 1989. Nuevos restos de mamíferos de la cuenca de Taubaté, Estado de Sao Paulo, Brasil. *Anais de la Academia Brasileira de Ciências*, **61**, 157–175.

Szalay, F. S. 1982. Phylogenetic relationships of the marsupials. *Geobios, Mémoire Special*, **6**, 177–190.

Szalay, F. S. 1994. *Evolutionary history of the marsupials and an analysis of osteological characters.* Cambridge University Press, Cambridge, 481 pp.

Thomas, R. H., **Schaffner W.**, **Wilson, A. C.** & **Pääbo, S.** 1989. DNA phylogeny of the extinct marsupial wolf. *Nature*, **340**, 465–467.

Van der Klaauw, C. J. 1931. The auditory bulla in some fossil mammals with a general introduction to this region of the skull. *Bulletin of the American Museum of Natural History*, **62**, 1–352.

Van Valkenburgh, B. 1988. Trophic diversity in past and present guilds of large predatory mammals. *Paleobiology*, **14**, 155–173.

Van Valkenburgh, B. 1989. Carnivore dental adaptations and diet: a study of trophic diversity within guilds. Pp. 410–436 in J. L. Gittleman (ed.) *Carnivore behaviour, ecology, and evolution*. Cornell University Press, Ithaca.

Van Valkenburgh, B. 1991. Iterative evolution of hypercarnivory in canids (Mammalia: Carnivora): evolutionary interactions among sympatric predators. *Paleobiology*, **17**, 340–362.

Van Valkenburgh, B. 1999. Major patterns in the history of carnivorous mammals. *Annual Review of Earth and Planetary Sciences*, **27**, 463–493.

Van Valkenburgh, B. 2007. Déjà vu: the evolution of feeding morphologies in the Carnivora. *Integrative and Comparative Biology*, **47**, 147–163.

Villarroel, C. & **Marshall, L. G.** 1982. Geology of the Deseadan (early Oligocene) age estratos Salla in the Salla-Luribay Basin, Bolivia with description of new Marsupialia. *Geobios, Mémoire Spécial*, **6**, 201–211.

Werdelin, L. 1987. Jaw geometry and molar morphology in marsupial carnivores: analysis of a constraint and its macroevolutionary consequences. *Paleobiology*, **13**, 342–350.

Werdelin, L. 1989. Constraint and adaptation in the bone-cracking canid *Osteoborus* (Mammalia: Canidae). *Paleobiology*, **15**, 387–401.

Wible, J. R. 2003. On the cranial osteology of the short-tailed opossum *Monodelphis brevicaudata* (Didelphidae, Marsupialia). *Annals of Carnegie Museum*, **72**, 137–202.

Wible, J. R. & **Rougier, G. W.** 2000. The cranial anatomy of *Kryptobaatar dashzevegi* (Mammalia, Multituberculata), and its bearing on the evolution of mammalian characters. *Bulletin of the American Museum of Natural History*, **247**, 1–124.

Zimicz, A. N. 2012. *Ecomorfología de los marsupiales paleógenos de América del Sur*. Unpublished PhD thesis, Universidad Nacional de La Plata, 454 pp.